AD-A098 913 OKLAHOMA UNIV NORMAN F/G 11/4
ANALYSIS OF LAYERED COMPOSITE PLATES ACCOUNTING FOR LARGE DEFLE--ETC(U)
MAY 81 J N REDDY N00014-78-C-0647
UNCLASSIFIED NL

END
DATE FILMED
6-81
DTIC

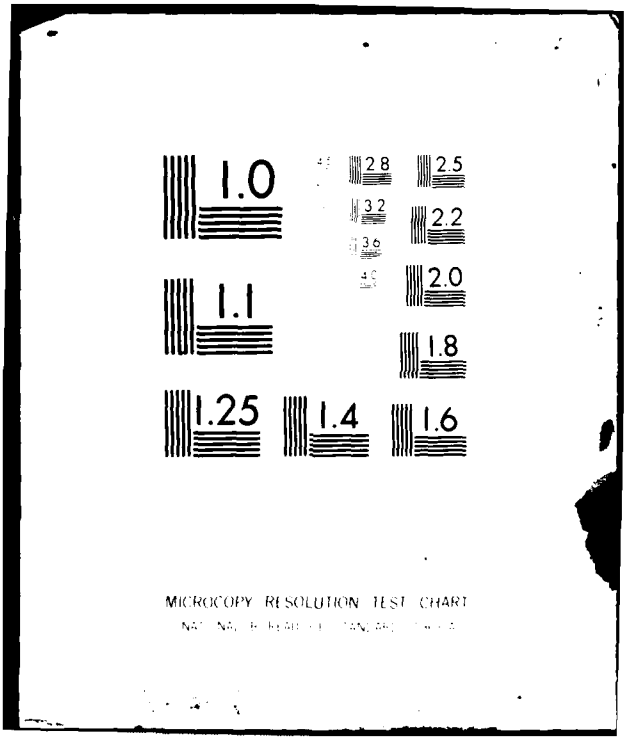
1.0
2.8
2.5
3.2
2.2
3.6
2.0
1.1
1.8
1.25
1.4
1.6
MICROCOPY RESOLUTION TEST CHART

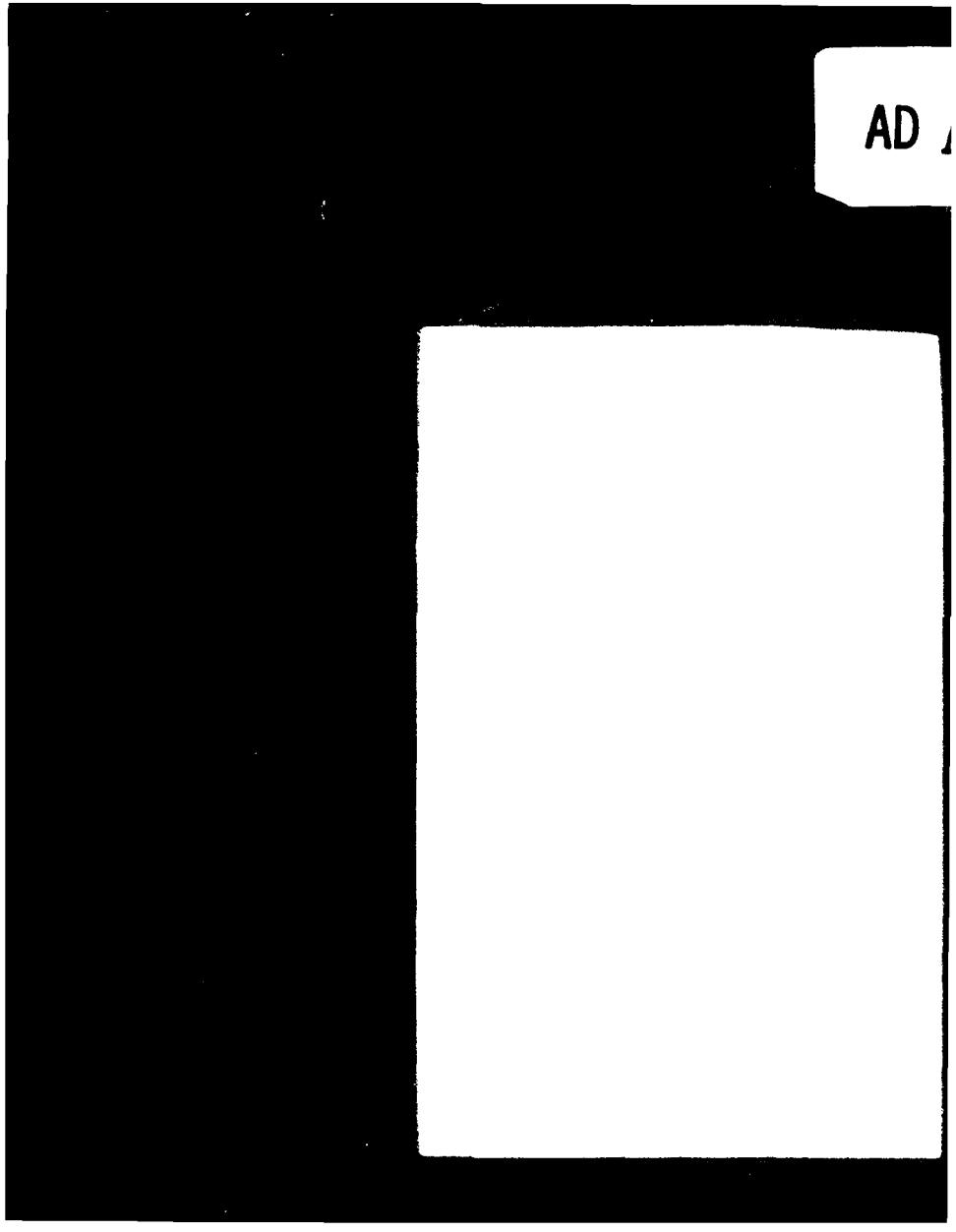
AD

LEVEL II

(12)

Department of the Navy
OFFICE OF NAVAL RESEARCH
Structural Mechanics Program
Arlington, Virginia 22217

Contract N00014-78-C-0647
Project NR 064-609
Technical Report No. 21

Report VPI-E-81-12

ANALYSIS OF LAYERED COMPOSITE PLATES ACCOUNTING FOR LARGE DEFLECTIONS AND TRANSVERSE SHEAR STRAINS

by

J. N. Reddy
Department of Engineering Science and Mechanics
Virginia Polytechnic Institute and State University
Blacksburg, Virginia, USA 24061

April 1981

Approved for public release; distribution unlimited

ANALYSIS OF LAYERED COMPOSITE PLATES ACCOUNTING FOR LARGE DEFLECTIONS AND TRANSVERSE SHEAR STRAINS

J. N. Reddy

Department of Engineering Science and Mechanics
Virginia Polytechnic Institute and State University
Blacksburg, VA 24061 USA
April, 1981

This paper is prepared for
RECENT ADVANCES IN NONLINEAR COMPUTATIONAL MECHANICS
edited by E. Hinton, C. Taylor, and D. R. J. Owen
Pine Ridge Press, Swansea, United Kingdom

A

ANALYSIS OF LAYERED COMPOSITE PLATES ACCOUNTING FOR LARGE DEFLECTIONS AND TRANSVERSE SHEAR STRAINS

J. N. Reddy

Department of Engineering Science and Mechanics
Virginia Polytechnic Institute and State University
Blacksburg, VA 24061 USA

1. INTRODUCTION

In recent years composites, especially fiber-reinforced laminates, have found increasing application in many engineering structures. This is mainly due to two desirable features of fiber-reinforced composites: (i) the high stiffness-to-weight ratio, and (ii) the anisotropic material property that can be tailored through variation of the fiber orientation and stacking sequence of lamina - a feature that gives the designer an added degree of flexibility. The increased use of fiber-reinforced composites as structural elements has generated considerable interest in the analysis of lamianted (anisotropic) composite plates.

Recent developments in the analysis of plates laminated of fiber-reinforced materials indicate that the plate thickness has more pronounced effect on the behavior of composite plates than isotropic plates. The classical thin-plate theory (CPT) assumes that normals to the midsurface before deformation remain straight and normal to the midsurface after deformation, implying that thickness shear deformation effects are negligible. As a result, the natural frequencies, for example, calculated using the thin-plate theory are higher than those obtained by including the transverse shear deformation effects. Also, the transverse deflections predicted by the thin-plate theory are lower than those predicted by a shear deformable theory (SDT). Due to the low transverse shear modulus relative to the in-plane Young's moduli, the transverse shear deformation effects are even more pronounced in the composite plates. Thus a reliable prediction of the small deflection response characteristics of high modulus composite plates requires the use of shear deformable theories.

When the transverse deflections experienced by plates are not small in comparison with the plate thickness, the interaction between membane stresses and the (bending and shear) curvatures of the plate must be considered. The interaction results in midplane stretching, which leads to nonlinear terms in the equations of motion. Thus, a more acccurate prediction of deflections, stresses, and frequencies requires the solution of the plate equations that account for large deflections and thickness shear deformation.

The present paper is concerned with a review of recent developments in the finite-element analysis of layered composite plates. The paper presents a shear deformable theory that accounts for large rotations (in the von Karman sense), a finite element model of the equations, and finite element results (of linear and nonlinear theory) for static bending and free vibration of rectangular plates. The following brief review, which cites the papers that have appeared in the open literature on the linear and nonlinear bending and vibration of layered composite plates, provides a background for the present paper.

A number of shear deformable theories for laminated plates have been proposed to date. The first such theory for laminated isotropic plates is due to Stavsky [1]. The theory has been generalized to laminated anisotropic plates by Yang, Norris, and Stavsky [2]. The Yang-Norris-Stavsky (YNS) theory represents a generalization of Reissner-Mindlin plate theory for homogeneous, isotropic plates to arbitrarily laminated anisotropic plates and includes shear deformation and rotatory inertia effects. A review of various other theories, for example, the effective stiffness theory of Sun and Whitney [3], the higher-order theory of Whitney and Sun [4], and the three-dimensional elasticity theory of Srinivas et al. [5-7], can be found in the paper by Bert [8]. It has been shown (see, for example, [3,5,9-13]) that the YNS theory is adequate for predicting the overall behavior such as transverse deflections and natural frequencies (first few modes) of laminated anisotropic plates.

The first application of the YNS theory is apparently due to Whitney and Pagano [14], who presented closed-form solutions for symmetric and antisymmetric cross-ply and angle-ply rectangular plates under sinusoidal load distribution and for free vibration of antisymmetric angle-ply rectangular plates. Fortier and Rosettos [15] analyzed free vibration of thick rectangular plates of unsymmetric cross-ply construction while Sinha and Rath [16] considered both vibration and buckling for the same type of plates. Following Whitney and Pagano [14], Bert and Chen [17] presented closed-form solution for the free vibration of simply supported rectangular plates of antisymmetric angle-ply laminates.

Finite-element analysis of layered composite plates began with the works of Pryor and Barker [18], and Barker, Lin and Dana [19], who employed an element with seven degrees of freedom (three displacements, two rotations and two shear slopes) per node to analyze thick laminated plates. Mau, Tong, and Pian [20], and Mau and Witmer [21] employed the so-called hybrid-stress finite element method to analyze thick composite plates. Using finite element models based on a form of Reissner's plate theory (i.e., 'mixed' formulation), Noor and Mathers [22,23] studied the effects of shear deformation and anisotropy on the response of lamiated anisotropic plates. One of the elements used by the authors (see [22]) possesses eighty degrees of freedom per element, and one cannot afford to use it without the luxury of having the enormous computational resources the authors had. Hinton [24,25] employed the so-called finite strip method to study the flexure and free vibration of layered cross-ply plates. Mawenya and Davies [26], and Panda and Natarajan [27] used the quadratic shell element of Ahmad, Irons and Zienkiewicz [28] to analyze bending of thick multilayer plates. Using two hybrid-stress elements, Spilker, Chou, and Orringer [29] studied the static bending of layered composite plates. The number of degrees of freedom in one of the elements is proportional to the number of layers, and therefore the core storage and execution time requirements for the element increase rapidly with the number of layers in the plate. Recently, the present author developed a simple and efficient finite element based on the YNS theory [30]. The element contains three displacements and two shear slopes as degrees of freedom per node. The accuracy and convergence characteristics of the element were investigated in [31]. The element has been used successfully in the thermoelastic analysis of ordinary and bimodulus (i.e., different elastic properties in tension and compression) layered composite plates by the author and his colleagues [30-34].

Much of the previous research in the analysis of composite plates is limited to linear problems. This may have been due to the complexity of the nonlinear partial differential equation associated with the large-deflection theory of composite plates. Approximate solutions to the large-deflection theory (in von Karman's sense) of laminated composite plates were attempted by Whitney and Leissa [35], Bennett [36], Bert [37], Chandra and Raju [38,39], Zaghloul and Kennedy [40], Chia and Prabhakara [41,42], and Noor and Hartley [43]. Chandra and Raju [38,39], and Chia and Prabhakara [41,42] employed the Galerkin method to reduce the governing nonlinear partial differential equations to an ordinary differential equation in time for the mode shape; the perturbation technique was used to solve the resulting equation. Zaghloul and Kennedy [40] used a finite-difference successive iterative technique in their analysis. In all of

these studies, with the exception of [43], the transverse shear effects were neglected. The finite element employed by Noor and Hartley [43] includes the effect of transverse shear strains; however, it is algebraically complex and involves a large degree of freedom per element and thus one can preclude the use of such elements in the nonlinear analysis of composite plates. Recently, the finite element developed in [30] by the author was extended to nonlinear bending of composite plates [44,45].

Analysis of nonlinear vibration of single-layer orthotropic plates was considered by Ambartsumyan [46], and Hassert and Nowinski [47]. Nowinski [48,49] analyzed rectilinearly orthotropic plates of circular and triangular planforms using Galerkin method. In these studies the effect of transverse shear deformation and rotatory inertia were not considered. Wu and Vinson [50] presented the dynamic analogue of Berger's equation of motion for an orthotropic plate, including the effect of transverse shear deformation and rotatory inetia; however, the solutions were restricted to only the transverse shear deformation. Mayberry and Bert [51] presented experimental as well as theoretical work on nonlinear vibration of laminated plates; however, the theoretical investigation was limited to single-layer specially orthotropic rectangular plate with all four edges clamped, and not including the effect of transverse shear deformation and rotatory inertia. Using an assumed mode shape and Galerkin method, Nowinski [52] presented a general equation for the nonlinear analysis (i.e., large deflection and large amplitude free vibration) of orthotropic plates (see also, Sathyamoorthy and Pandalai [53]). Prabhakara and Chia [54] presented an analytical investigation of the nonlinear vibration of a rectangular orthotropic plate with all simply supported and all clamped edges. The effect of transverse shear and rotatory inertia on large amplitude vibration of composite plates was reported recently by Sathyamoorthy and Chia [55-57] using Galerkin method and the Runge-Kutta numerical procedure.

Layered composite plates exhibit, in general, coupling between the in-plane displacements and the transverse displacement and shear rotations. For plates having layers stacked symmetrically with respect to the mid-plane, the bending-stretching coupling terms vanish and the problem becomes relatively simpler. Wu and Vinson [58] extended their earlier work [50] to deal with the nonlinear vibration of symmetrically stacked laminated composite plates. The first nonlinear vibration analysis of unsymmetrically laminated plates is due to Bennett [36], who considered simply supported (with immovable edges) angle-ply plates. Using the thin plate theory of layered composite plates and Galerkin method, Bert [37] investigated the nonlinear vibration of a rectangular plate arbitrarily laminated of anisotropic material. A

multimode (two-term) solution for nonlinear vibration of unsymmetric all-clamped and all-simply supported angle-ply and cross-ply laminated plates was reported by Chandra and Basava Raju [38,39,59]. Chandra [39] used a one-term Galerkin approximation for the dynamic von Karman plate equations and the perturbation technique for the resulting ordinary equation in time to investigate the large-amplitude vibration of a cross-ply plate which is simply supported at two opposite edges and clamped at the other two edges. Prabhakara and Chia [54] presented an analytical investigation of the nonlinear free flexural vibrations of unsymmetric cross-ply and angle-ply plates with all-clamped and all-simply supported edges. The normal and tangential boundary forces in the plane of the plate were assumed to be zero. In all of these studies, the effects of shear deformation and rotatory inertia were neglected, and only rectangular geometries were considered. The latter restriction is a direct result of the methods of analysis used (i.e., Galerkin method, perturbation method and the double series method cannot be applied to plates of complicated geometries). Recently, the present author [60] investigated the nonlinear vibration of layered composite plates using the finite element method.

2. GOVERNING EQUATIONS ([45,60])

Consider a (thick) plate of uniform thickness h, laminated of anisotropic layers with the material axes of each layer being arbitrarily oriented with respect to the midplane of the plate. The midplane of the plate, denoted by $\mathbb{R}$, forms the x-y plane of the coordinate system, with the z-axis perpendicular to the midplane of the plate. In order to account for the midplane stretching due to large deflections, the shear deformable theory of Whitney and Pagano [14] is modified to include large rotations (in the von Karman sense). The displacement field is assumed to be of the form,

$$\begin{aligned} u_1(x,y,z,t) &= u(x,y,t) + z\,\psi_x(x,y,t), \\ u_2(x,y,z,t) &= v(x,y,t) + z\,\psi_y(x,y,t), \\ u_3(x,y,z,t) &= w(x,y,t). \end{aligned} \tag{1}$$

Here t is the time; u_2, u_2, u_3 are the displacements in x, y, z directions, respectively; u, v, w are the associated midplane displacements; and ψ_x and ψ_y are the slopes in the xz and yz planes due to bending only. Assuming that the plate is moderately thick and strains are much smaller than rotations, the nonlinear strain-displacement relations can be expressed in the form,

$$\varepsilon_1 = \frac{\partial u}{\partial x} + \frac{1}{2}\left(\frac{\partial w}{\partial x}\right)^2 + z\,\frac{\partial \psi_x}{\partial x} \equiv \varepsilon_1^0 + z\kappa_1$$

$$\varepsilon_2 = \frac{\partial v}{\partial y} + \frac{1}{2}\left(\frac{\partial w}{\partial y}\right)^2 + z\frac{\partial \psi_y}{\partial y} \equiv \overset{0}{\varepsilon_2} + z\kappa_2$$

$$\varepsilon_6 = \frac{\partial u}{\partial y} + \frac{\partial v}{\partial x} + \frac{\partial w}{\partial x}\frac{\partial w}{\partial y} + z\left(\frac{\partial \psi_x}{\partial y} + \frac{\partial \psi_y}{\partial x}\right) \equiv \overset{0}{\varepsilon_6} + z\kappa_6$$

$$\varepsilon_5 = \psi_x + \frac{\partial w}{\partial x}\ , \quad \varepsilon_4 = \psi_y + \frac{\partial w}{\partial y} \tag{2}$$

wherein the products of ψ_x, ψ_y, $\partial u_1/\partial x$ and $\partial u_2/\partial y$ are neglected. Since the constitutive relations, to be given shortly, are based on the plane-stress assumption, strain ε_3 does not come into the equations.

Neglecting the body moments and surface shearing forces, we write the equations of motion (in the absence of surface and body forces) as,

$$\begin{aligned}
&N_{1,x} + N_{6,y} = Pu_{,tt} + R\psi_{x,tt}\\
&N_{6,x} + N_{2,y} = Pv_{,tt} + R\psi_{y,tt}\\
&Q_{1,x} + Q_{2,y} + N(N_i, w) = Pw_{,tt}\\
&M_{1,x} + M_{6,y} - Q_1 = I\psi_{x,tt} + Ru_{,tt}\\
&M_{6,x} + M_{2,y} - Q_2 = I\psi_{y,tt} + Rv_{,tt}
\end{aligned} \tag{3}$$

where P, R, and I are the normal, coupled normal-rotatory, and rotatory inertia coefficients,

$$(P,R,I) = \int_{-h/2}^{h/2} (1,z,z^2)\rho dz = \sum_m \int_{z_m}^{z_{m+1}} (1,z,z^2)\rho^{(m)} dz \tag{4}$$

$\rho^{(m)}$ being the material density of the m-th layer, N_i, Q_i, and M_i are the stress and moment resultants defined by

$$(N_i,M_i) = \int_{-h/2}^{h/2} (1,z)\sigma_i\, dz\ , \quad (Q_1,Q_2) = \int_{-h/2}^{h/2} (\sigma_5,\sigma_4)dz, \tag{5}$$

and $N(\cdot)$ is the nonlinear operator,

$$N(w,N_i) = \frac{\partial}{\partial x}\left(N_1 \frac{\partial w}{\partial x}\right) + \frac{\partial}{\partial y}\left(N_6 \frac{\partial w}{\partial x}\right) + \frac{\partial}{\partial x}\left(N_6 \frac{\partial w}{\partial y}\right) + \frac{\partial}{\partial y}\left(N_2 \frac{\partial w}{\partial y}\right)$$

Here σ_i ($i = 1,2...6$) denotes the in-plane stress components ($\sigma_1 = \sigma_x$, $\sigma_2 = \sigma_y$, $\sigma_4 = \sigma_{yz}$, $\sigma_5 = \sigma_{xz}$ and $\sigma_6 = \sigma_{xy}$).

Assuming the existence of one plane of elastic symmetry parallel to the plane of each layer, the constitutive equations for the m-th layer (in the plate coordinates) are given by

$$\begin{Bmatrix}\sigma_1\\ \sigma_2\\ \sigma_6\end{Bmatrix} = [Q_{ij}^{(m)}]\begin{Bmatrix}\varepsilon_1\\ \varepsilon_2\\ \varepsilon_6\end{Bmatrix}, \quad \begin{Bmatrix}\sigma_4\\ \sigma_5\end{Bmatrix} = \begin{bmatrix}Q_{44}^{(m)} & Q_{45}^{(m)}\\ Q_{45}^{(m)} & Q_{55}^{(m)}\end{bmatrix}\begin{Bmatrix}\varepsilon_4\\ \varepsilon_5\end{Bmatrix}, \quad (6)$$

where $Q_{ij}^{(m)}$ are the stiffness coefficients of the m-th layer in the plate coordinates. Combining eqns. (5) and (6), we obtain the plate constitutive equations,

$$\begin{Bmatrix}N_i\\ M_i\end{Bmatrix} = \begin{bmatrix}A_{ij} & B_{ij}\\ B_{ji} & D_{ij}\end{bmatrix}\begin{Bmatrix}\varepsilon_j^0\\ \kappa_j\end{Bmatrix}, \quad \begin{Bmatrix}Q_2\\ Q_1\end{Bmatrix} = \begin{bmatrix}A_{44} & A_{45}\\ A_{45} & A_{55}\end{bmatrix}\begin{Bmatrix}\varepsilon_4\\ \varepsilon_5\end{Bmatrix} \quad (7)$$

The A_{ij}, B_{ij}, D_{ij} (i,j = 1,2,6), and A_{ij} (i,j = 4,5) are the respective inplane, bending-plane coupling, bending or twisting, and thickness-shear stiffnesses, respectively:

$$(A_{ij},B_{ij},D_{ij}) = \sum_m \int_{z_m}^{z_{m+1}} Q_{ij}^{(m)}(1,z,z^2)dz \quad ,$$

$$A_{ij} = \sum_m \int_{z_m}^{z_{m+1}} k_i k_j Q_{ij}^{(m)} dz. \quad (8)$$

Here z_m denotes the distance from the mid-plane to the lower surface of the m-th layer, and k_i are the shear correction coefficients.

Equations (3) and (7) must be adjoined by appropriate boundary conditions of the problem. The variational formulation of these equations indicate the following essential and natural boundary conditions:

$$\begin{aligned}&\underline{\text{essential}}: \quad \text{specify, } u_n,\ u_s,\ w,\ \psi_n,\ \psi_s,\\ &\underline{\text{natural}}: \quad \text{specify, } N_n,\ N_{ns},\ q,\ M_n,\ M_{ns}.\end{aligned} \quad (9)$$

wherein u_n and u_s, for example, denote the normal and tangential components of the in-plane displacement vector, $u = (u,v)$.

3. FINITE ELEMENT MODEL ([44,45,60])

The equations presented in the previous section are valid for any arbitrarily laminated composite plate. Except under certain special conditions of geometry, boundary conditions and stacking of layers, these equations do not admit exact solutions (in fact, exact closed-form solutions cannot be

obtained without invoking small-displacement assumption; see [29]). Here we present a finite-element model associated with the equations governing the nonlinear analysis of layered composite plates. The element is an extension of the penalty plate-bending element developed for the linear analysis of layered composite plates by the author [28,29].

Consider a finite-element analogue, $\bar{\mathbb{R}}$, of the midplane of the plate, $\mathbb{R}$. Over a typical element $\mathbb{R}_e$ of the mesh $\bar{\mathbb{R}}$ a typical generalized displacement, U, is interpolated in space by expression of the form,

$$U = \sum_{i}^{n} U_i \phi_i \tag{10}$$

where U_i is the value of U at node i, ϕ_i is the finite-element interpolation function at node i and n is the number of nodes in the element. For simplicity, we use the same interpolation for each of the generalized displacements.

The weak form of eqns. (3) and (7) over a typical element is given by

$$\begin{aligned} 0 = \int_{\mathbb{R}^e} & \{\delta u(Pu_{,tt}+R\psi_{x,tt})+\delta u_{,x}N_1+\delta u_{,y}N_6+\delta v(Pv_{,tt}+R\psi_{y,tt}) \\ & + \delta v_{,x}N_6+\delta v_{,y}N_2+\delta w\, Pw_{,tt})+\delta w_{,x}Q_1+\delta w_{,y}Q_2 \\ & + \frac{\partial \delta w}{\partial x}\frac{\partial w}{\partial x}N_1+\frac{\partial \delta w}{\partial y}\frac{\partial w}{\partial x}N_6+\frac{\partial \delta w}{\partial x}\frac{\partial w}{\partial y}N_6+\frac{\partial \delta w}{\partial y}\frac{\partial w}{\partial y}N_2 \\ & + \delta\psi_x(I\psi_{x,tt}+Ru_{,tt})+\delta\psi_{x,x}M_1+\delta\psi_{x,y}M_6+\delta\psi_x Q_1 \\ & + \delta\psi_y(I\psi_{y,tt}+Rv_{,tt})+\delta\psi_{y,x}M_6+\delta\psi_{y,y}M_2+\delta\psi_y Q_2\}\, dxdy \\ & + \int_{C_n}(\delta u_n N_n+\delta u_s N_{ns})ds+\int_{C_q}\delta w q ds+\int_{C_m}(\delta\psi_n M_n+\delta\psi_s M_{ns})ds, \end{aligned} \tag{11}$$

where N_i, M_i, and Q_i are given in terms of the generalized displacements by eqn. (7). The boundary terms N_n, N_{ns}, q, M_n, and M_{ns} (notation used is very standard) in eqn. (11) get cancelled at interelement boundaries, and equal to those specified at the plate boundary.

Let u, v, w, ψ_x, and ψ_y be approximated over each element by

$$u = U\tau(t),\ v = V\tau(t),\ w = W\lambda(t),\ \psi_x = X\mu(t),\ \psi_y = Y\mu(t) \tag{12}$$

where U, V, etc., are given by ean. (10), and $\tau(t)$, $\lambda(t)$, and $\mu(t)$ are time dependent functions whose specific form is to

be determined. Substituting eqns. (10) and (12) into eqn. (11), we obtain the following element equation:

$$[K]\{\Delta\} + [M]\{\Delta\} = \{F\} \tag{13}$$

Here $\{\Delta\}$ is the column vector of the nodal values of the generalized displacements, $[K]$ is the matrix of stiffness coefficients (which depends on the generalized displacements), $[M]$ is the matrix of mass coefficients, and $\{F\}$ is the column vector containing the boundary contributions. The elements of $[K]$ and $[M]$ are given in Appendix B. It should be noted from $[K]$ in the appendix that the time functions are not harmonic. That is, strictly speaking, eqn. (13) must be solved as one of transient equation (even in the case of free vibrations). However, in the present analysis we assume, for simplicity, that

$$\tau = \mu = \lambda^2 = \cos^2 \omega t \tag{14}$$

and retain only the first term of the cosine series. This assumption yields the standard eigenvalue problem in the case of natural vibration:

$$([K] - \omega^2[M])\{\Delta\} = \{0\}. \tag{15}$$

The solution procedure consists of a direct iteration, in which the global stiffness $[K]$ is updated using the global displacement (eigen function) vector $\{\Delta\}$ from the previous iteration. If $\{\Delta\}$ is set to zero (as was done in the present analysis) at the beginning of the iteration procedure, we obtain the linear solution (frequencies) of the problem at the end of the first iteration. The iteration is terminated when the nonlinear solution (frequencies) obtained during two consecutive iterations differ by some small number (say, one percent).

In the present study linear (4-node) and quadratic (8-node and 9-node) isoparametric elements are employed. The element stiffness matrices are of the order 20 x 20, 40 x 40, and 45 x 45 respectively.

As pointed out in [30,61], the shear deformable theory presented herein can be derived from the classical thin plate theory by using the penalty function method to incorporate the slope-displacement relations

$$\frac{\partial w}{\partial x} = -\theta_x \quad , \quad \frac{\partial w}{\partial y} = -\theta_y$$

as constraints into the variational formulation of the thin plate theory. It is well-known that reduced integration must be used in the numerical solution of penalty function problems. In other words, the shear energy terms (which correspond to the penalty functional) in the element matrices

must be underintegrated. This means that a 1x1 Gauss rule must be used in place of the standard 2x2 Gauss rule in the evaluation of the stiffness coefficients associated with the shear energy for the four-node element. For more details on the reduced integration in plates, see [62,63].

6. NUMERICAL RESULTS AND DISCUSSION

The finite element presented herein was employed in the nonlinear analysis of rectangular plates. The following material properties typical of advanced fiber-reinforced composites were used in the present study:

$$\text{Material I: } E_1/E_2=25,\ G_{12}/E_2=0.5,\ G_{22}/E=0.2,\ \nu_{12}=0.25$$

$$\text{Material II: } E_1/E_2=40,\ G_{12}/E_2=0.6,\ G_{23}/E_2=0.5,\ \nu_{12}=0.25 \tag{16}$$

It is assumed that $G_{13} = G_{23}$ and $\nu_{12} = \nu_{13}$. A value of 5/6 was used for the shear correction coefficients, $k_4^2=k_5^2$ (see Whitney [64]). All of the computations were carried on an IBM 370/158 computer in double precision.

6.1 Static Bending Results ([30,31,44,45]).

To show the effect of the reduced integration, and to illustrate the accuracy of the present element, results of the linear analysis are presented. Numerical experiments were conducted to investigate the effect of element type (i.e., linear, eight-node quadratic, and nine-node quadratic), mesh (L2 = linear 2 by 2, Q2 = 2Q8 = 8-node quadratic 2 by 2 elements in quarter plate), and reduced integration on the deflections and stresses.

In Table 1 linear and quadratic elements are compared for deflections and stresses of a three-layer ($h_1 = h_3 = h/4$, $h_2 = h/2$) square plate (material I) subjected to sinusoidal loading. This problem is also equivalent to a four-layer (equal thickness) cross-ply laminate. The following boundary conditions were used (in the finite element method only the essential boundary conditions were imposed):

$$\begin{aligned}
&u_0(x,0) = u_0(x,b) = 0,\ N_2(x,0) = N_2(x,b) = 0\\
&v_0(0,y) = v_0(a,y) = 0,\ N_1(0,y) = N_1(a,y) = 0\\
\text{SS-1:}\quad &w(x,0) = w(x,b) = w(0,y) = w(a,y) = 0\\
&\psi_x(x,0) = \psi_x(x,b) = 0,\ M_2(x,0) = M_2(x,b) = 0\\
&\psi_y(0,y) = \psi_y(a,y) = 0,\ M_1(0,y) = M_1(a,y) = 0
\end{aligned} \tag{17}$$

be determined. Substituting eqns. (10) and (12) into eqn. (11), we obtain the following element equation:

$$[K]\{\Delta\} + [M]\{\Delta\} = \{F\} \tag{13}$$

Here $\{\Delta\}$ is the column vector of the nodal values of the generalized displacements, $[K]$ is the matrix of stiffness coefficients (which depends on the generalized displacements), $[M]$ is the matrix of mass coefficients, and $\{F\}$ is the column vector containing the boundary contributions. The elements of $[K]$ and $[M]$ are given in Appendix B. It should be noted from $[K]$ in the appendix that the time functions are not harmonic. That is, strictly speaking, eqn. (13) must be solved as one of transient equation (even in the case of free vibrations). However, in the present analysis we assume, for simplicity, that

$$\tau = \mu = \lambda^2 = \cos^2 \omega t \tag{14}$$

and retain only the first term of the cosine series. This assumption yields the standard eigenvalue problem in the case of natural vibration:

$$([K] - \omega^2[M])\{\Delta\} = \{0\}. \tag{15}$$

The solution procedure consists of a direct iteration, in which the global stiffness $[K]$ is updated using the global displacement (eigen function) vector $\{\Delta\}$ from the previous iteration. If $\{\Delta\}$ is set to zero (as was done in the present analysis) at the beginning of the iteration procedure, we obtain the linear solution (frequencies) of the problem at the end of the first iteration. The iteration is terminated when the nonlinear solution (frequencies) obtained during two consecutive iterations differ by some small number (say, one percent).

In the present study linear (4-node) and quadratic (8-node and 9-node) isoparametric elements are employed. The element stiffness matrices are of the order 20 x 20, 40 x 40, and 45 x 45 respectively.

As pointed out in [30,61], the shear deformable theory presented herein can be derived from the classical thin plate theory by using the penalty function method to incorporate the slope-displacement relations

$$\frac{\partial w}{\partial x} = -\theta_x \quad , \quad \frac{\partial w}{\partial y} = -\theta_y$$

as constraints into the variational formulation of the thin plate theory. It is well-known that reduced integration must be used in the numerical solution of penalty function problems. In other words, the shear energy terms (which correspond to the penalty functional) in the element matrices

The stresses were computed at the Gaussian points (see Fig. 1):

$$\bar{w} = \frac{w(\frac{a}{2},\frac{a}{2},0)E_2h^3 \times 10^3}{q_0a^4}, \quad \bar{\sigma}_x = (\frac{h}{a})^2 \frac{1}{q_0} \sigma_x(A,A,\pm t/2),$$

$$\bar{\sigma}_y = (\frac{h}{a})^2 \frac{1}{q_0} \sigma_y(A,A,\pm t/4), \quad \bar{\tau}_{xy} = (\frac{h}{a})^2 \frac{1}{q_0} \tau_{xy}(B,B,\pm t/2) \quad (18)$$

$$\bar{\tau}_{xz} = \frac{h}{aq_0} \tau_{xz}(B,A) \text{ in layers 1 \& 3; } \bar{\tau}_{yz} = \frac{h}{aq_0} \tau_{yz}(A,B)$$

in layer 2 where A and B are the Gauass-point coordinates (as a fraction of sides a and b) given below:

	2x2 linear	4x4 linear	2x2 quadratic	4x4 quadratic
A	0.125	0.0625	0.05283	0.02642
B	0.375	0.4375	0.4472	0.4736

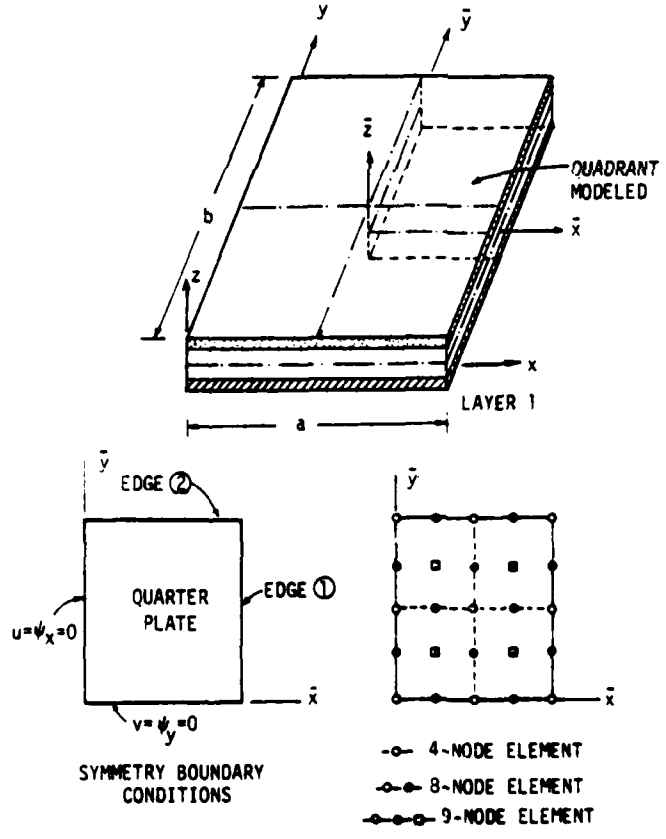

Figure 1. Laminated plate geometry, boundary conditions, and finite element discretization by linear and quadratic elements.

Table 1 Effect of reduced integration on the maximum deflection and stresses of a three-ply (0°/90°/0°) square plate subjected to sinusoidal loading ($h_1=h_3=h/4$, $h_2=h/2$, material I).

a/h	Source	$\bar{w}$	$\bar{\sigma}_x$	$\bar{\sigma}_y$	$\bar{\tau}_{xy}$	$\bar{\tau}_{xz}$	$\bar{\tau}_{yz}$
10	3-DES [11]	7.434	0.599	0.403	0.0276	0.301	0.196
	CFS [31]	6.627	0.496	0.359	0.0240	0.414	0.128
	Ref. [27]	6.299	0.532	0.307	0.0250	--	--
	4Q8-R	6.627	0.495	0.359	0.0240	0.414	0.128
	4L-R	6.599	0.467	0.347	0.0227	0.395	0.208
	4L-F	6.427	0.451	0.328	0.0219	347.5	247.2
	2Q8-R	6.615	0.484	0.351	0.0234	0.404	0.126
	2Q8-F	6.605	0.483	0.349	0.0234	0.404	0.126
	2Q9-R	6.561	0.480	0.341	0.0231	0.400	0.126
	2Q9-F	6.551	0.479	0.340	0.0231	0.399	0.126
	2Q9-FR	6.558	0.480	0.341	0.0230	0.400	0.126
	2L-R	6.508	0.380	0.284	0.0187	0.355	0.107
	2L-F	5.901	0.334	0.245	0.0163	261.6	261.4
20	3-DES [11]	5.173	0.543	0.308	0.0230	0.328	0.156
	CFS [31]	4.911	0.524	0.294	0.0219	0.434	0.108
	Ref. [27]	4.847	0.557	0.307	0.0231	--	--
	4Q8-R	4.911	0.524	0.294	0.0219	0.434	0.108
	4L-R	4.863	0.494	0.278	0.0207	0.415	0.103
	4L-F	4.346	0.437	0.245	0.0183	115.5	115.3
	2Q8-R	4.091	0.511	0.287	0.0214	0.424	0.106
	2Q8-F	4.876	0.508	0.284	0.0214	0.424	0.106
	2Q9-R	4.847	0.505	0.278	0.0213	0.418	0.106
	2Q9-F	4.827	0.502	0.275	0.0211	0.418	0.107
	2Q9-FR	4.847	0.505	0.278	0.0212	0.417	0.106
	2L-R	4.712	0.404	0.229	0.0170	0.353	0.089
	2L-F	3.236	0.265	0.149	0.0111	70.55	70.4
100	3-DES [11]	4.385	0.539	0.271	0.0214	0.339	0.139
	CFS [31]	4.337	0.535	0.269	0.0212	0.442	0.100
	Ref. [27]	4.363	0.566	0.284	0.0223	--	--
	4Q8-R	4.336	0.535	0.269	0.0212	0.442	0.100
	4L-R	4.281	0.505	0.254	0.0200	0.422	0.096
	4L-F	1.034	0.120	0.060	0.0048	9.327	9.404
	2Q8-R	4.319	0.521	0.262	0.0206	0.435	0.102
	2Q8-F	4.143	0.490	0.244	0.0199	0.430	0.100
	2Q9-R	4.301	0.418	0.255	0.0207	0.428	0.099
	2Q9-F	4.158	0.490	0.242	0.0201	0.427	0.100
	2Q9-FR	4.299	0.518	0.255	0.0206	0.426	0.099
	2L-R	4.107	0.413	0.208	0.0164	0.356	0.082
	2L-F	0.315	0.003	0.015	0.0012	2.173	2.192
classical thin-plate solution		4.350	0.539	0.269	0.213	0.339	0.138

In Table 1, R denotes reduced integration, F = full integration, and FR = full integration for bending terms, and reduced integration for the shear terms. The following observations can be made from the results of Table 1.

1. The nine-node element gives virtually the same results for full (3x3 Gauss rule), reduced (2x2 Gauss rule), and mixed (3x3 and 2x2 Gauss rules) integrations. However, the results attained by using the reduced integration are the closest of all three integrations to the closed-form solution [31].

2. The nine-node element and the eight-node element (with reduced integration) give almost identical results (contrary to the belief that the nine-node element is superior to the eight-node element) for all side-to-thickness ratios.

3. Integration rule has a more profound effect on the accuracy in the eight-node element than in the nine-node element. Full integration gives less accurate results than the reduced integration, and the error increases with the side-to-thickness ratio. This implies that the reduced integration is a must for thin plates, as generally recognized for all penalty-function based finite element models.

4. Full integration results in, relatively, smaller errors for quadratic elements and for refined meshes than for linear elements and/or for coarse meshes. That is, the error between the solutions obtained by 2Q8-F and 2Q8-R is smaller than those obtained by 4L-F and 4L-R, and the error between the solutions obtained by 4L-F and 4L-R is smaller than those obtained by 2L-F and 2L-R.

5. Numerical convergence of the element is clear from the results.

It should be pointed out that the present finite-element solutions are not expected to agree exactly with the 3-D elasticity solution, because the element is based on the YNS theory rather than the 3-D elasticity equations. The accuracy of the YNS theory is evident from the results. While the YNS theory seems to predict the maximum deflection very close to that given by the 3-D elasticity solution, the stresses, especially the transverse shear stresses, are not in good agreement for thick plates. The stresses predicted by the YNS theory are on the lower side of the 3-D elasticity results.

In the results to be presented, reduced integration was used with linear and quadratic elements.

Table 2 Comparison of maximum deflection and stressesof a three-ply (0°/90°/0°) square plate subjected to sinusoidal loading (h_i = h/3, material I).

a/h	Source		$0.1\bar{w}$	$\bar{\sigma}_x$	$\bar{\sigma}_y$	$\bar{\tau}_{xy}$	$\bar{\tau}_{xz}$	$\bar{\tau}_{yz}$
10	Pagano [10]		-	0.590	0.288	0.029	0.357	0.123
	closed-form solution [31]		0.669	0.510 0.499	0.252 0.247	0.0250 0.0243	0.406 0.396	0.091* 0.089
	Present	4Q8-R	0.669	0.510	0.252	0.0250	0.406	0.091
	FEM	2Q8-R	0.668	0.498	0.249	0.0244	0.397	0.089
20	Pagano [10]		-	0.552	0.210	0.0234	0.385	0.094
	closed-form solution [31]		0.482	0.528 0.517	0.198 0.194	0.0222 0.0216	0.418 0.408	0.075 0.074
	FEM	4Q8-R	0.492	0.528	0.198	0.0222	0.418	0.075
		2Q8-R	0.491	0.516	0.194	0.0217	0.408	0.074
50	Pagano [10]		-	0.541	0.185	0.0216	0.393	0.084
	closed-form solution [31]		0.441	0.534 0.523	0.182 0.178	0.0213 0.0207	0.421 0.412	0.071 0.069
	FEM	4Q8-R	0.441	0.534	0.182	0.0213	0.421	0.071
		2Q8-R	0.440	0.521	0.178	0.0208	0.412	0.070
100	Pagano [10]		-	0.539	0.181	0.0213	0.395	0.083
	closed-form solution [31]		0.434	0.535 0.524	0.179 0.176	0.0212 0.0206	0.422 0.412	0.070 0.068
	FEM	4Q8-R	0.434	0.535	0.179	0.0212	0.422	0.070
		2Q8-R	0.432	0.522	0.175	0.0207	0.416	0.068
	classical plate theory [10]		-	0.539	0.180	0.0213	0.395	0.082

*The first row of stresses is for 4x4 Gauss points and the second row is for 2x2 Gauss points.

In Table 2, the 3-D elasticity solution of Pagano [10] the closed-form solution [31] and 4Q8 and 2Q8 finite-element results (FEM) are compared for three-layer (0°/90°/0°), equal thickness, square plate (material I). The present finite-element results are in excel agreement with the closed-form solution of the equations governing the YNS theory. The stresses in 3-D elasticity solution were reported to be maximum at the following points:

$$\bar{\sigma}_x = \bar{\sigma}_x(\tfrac{a}{2},\tfrac{b}{2},\pm h/2) \quad , \quad \bar{\sigma}_y = \bar{\sigma}_y(\tfrac{a}{2},\tfrac{b}{2},\pm h/4) \quad , \quad \bar{\tau}_{xy} = \bar{\tau}_{xy}(a,b,\tfrac{h}{2})$$

$$\bar{\tau}_{xz} = \bar{\tau}_{xz}(a,\tfrac{b}{2},0) \quad , \quad \bar{\tau}_{yz} = \bar{\tau}_{yz}(\tfrac{a}{2},b,0) \qquad (20)$$

Table 3 compares the maximum deflection and stresses in a three-layer ($h_1 = h_3 = 0.1h$, $h_2 = 0.8h$), square sandwich plate (0°/90°/0°) subjected to sinusoidal loading. The material of

Table 3 Comparison of maximum deflection and stresses in a three-layer sandwich (0°/90°/0°) plate subjected to sinusoidal loading (h_1=h_3=0, h_2=0.8h, material I, 2Q8-R).

a/h	source	$\bar{w}$	$\bar{\sigma}_x$	$\bar{\sigma}_y$	$\bar{\tau}_{xy}$	$\bar{\tau}_{xz}$	$\bar{\tau}_{yz}$
	3-DES [10]	-	3.278	0.4517	0.2403	0.185	0.140
2	CFS	9.552	0.718	0.3622	0.1954	0.876	0.252
	FEM	9.543	0.716	0.3615	0.1961	0.877	0.253
	3-DES [10]	-	1.556	0.2595	0.1437	0.239	0.107
4	CFS	4.7672	0.867	0.1520	0.0877	0.993	0.174
	FEM	4.7606	0.865	0.1517	0.8781	0.994	0.174
	3-DES [10]	-	1.153	0.1104	0.0707	0.300	0.053
10	CFS	1.560	1.017	0.0776	0.0533	1.110	0.095
	FEM	1.558	1.015	0.0774	0.0535	1.112	0.095
	3-DES [10]	-	1.110	0.0700	0.0511	0.317	0.036
20	CFS	1.0524	1.053	0.0595	0.0450	1.140	0.076
	FEM	1.0503	1.051	0.0594	0.0452	1.140	0.076
	3-DES [10]	-	1.064	0.0541	0.0425	0.323	0.031
50	CFS	0.9064	1.065	0.0539	0.0424	1.148	0.070
	FEM	0.9040	1.062	0.0538	0.0425	1.151	0.071
	3-DES [10]	-	1.098	0.0550	0.0437	0.324	0.029
100	CFS	0.8852	1.067	0.0531	0.0420	1.149	0.069
	FEM	0.8822	1.063	0.0530	0.0421	1.158	0.072
	CPT	-	1.097	0.0534	0.0433	0.324	0.029

the face sheets (i.e., layers 1 and 3) is the same as material I, and the core material is transversely isotropic with respect to z and is characterized by the following properties (see Pagano [10]),

$$E_1/E_2 = 1.0 \quad , \quad E_3/E_2 = 12.5 \text{ (not used in YNS theory)} \tag{21}$$

$$G_{13}/G_{23}=1.5E_2 \quad , \quad G_{12}=0.4\ E_2 \quad , \quad \nu_{12}=\nu_{13}=\nu_{23}=0.25$$

The finite-element results are in good agreement with the closed-form solution; however, the YNS theory seems to predict the stresses quite low for thick plates.

Figure 2 shows the nondimensionalized deflection versus side-to-thickness ratio for two, four and sixteen layer angle-ply (45°/-45°/+/-/...) square plates (material II) under sinusoidal loading. The following edge conditions were employed:

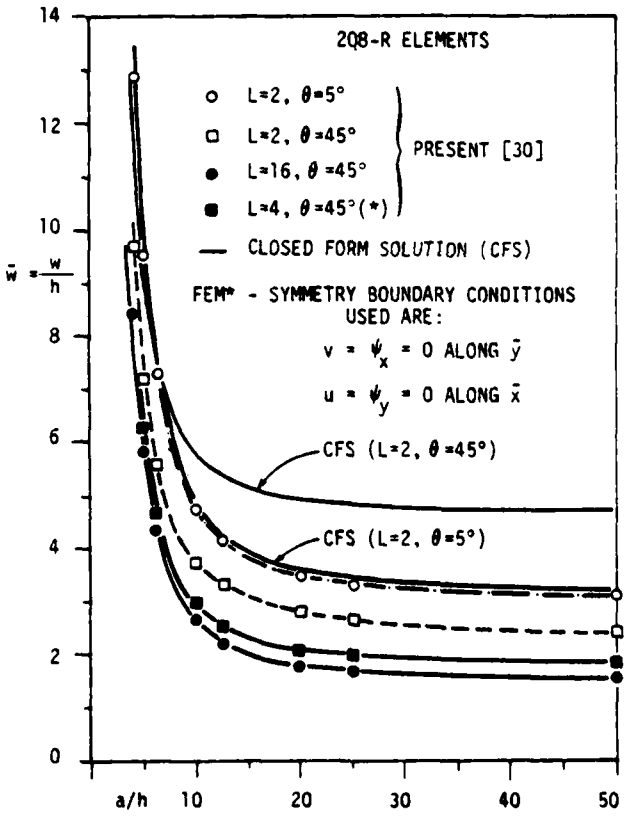

Figure 2. Nondimensionalized deflection versus side-to-thickness ratio for simply-supported (SS-2) angle-ply plates under sinusoidal loading (material II).

$$u_0(0,y) = u_0(a,y) = 0 \quad , \quad N_6(0,y) = N_6(a,y) = 0$$

$$v_0(x,0) = v_0(x,b) = 0 \quad , \quad N_6(x,0) = N_6(x,b) = 0$$

$$\text{SS-2:} \quad w(x,0) = w(x,b) = w(0,y) = w(a,y) = 0 \qquad (22)$$

$$\psi_x(x,0) = \psi_x(x,b) = 0 \quad , \quad M_2(x,0) = M_2(x,b) = 0$$

$$\psi_y(0,y) = \psi_y(a,y) = 0 \quad , \quad M_1(0,y) = M_1(a,y) = 0$$

Dark lines and symbols correspond, respectively, to the closed-form solution and the finite-element solution (with the symmetry conditions of the CFS imposed). The finite element solutions are in excellent agreement with the closed form solution.

Having established the credibility of the finite element presented herein for the linear analysis of layered composite plates, we now employ the element in the nonlinear analyses. First, results are presented for single-layer isotropic square plates under uniform loading. The essential boundary conditions used are (BC3 and BC5 in Table 4):

simply-supported (SS-3): $u=v=w=0$ on all edges. (22)

clamped (CC-1):
$$\begin{cases} u=v=w=0 \text{ on all edges,} \\ \psi_y=0 \text{ along edges parallel to x-axis,} \\ \psi_x=0 \text{ along edges parallel to y-axis.} \end{cases} \qquad (23)$$

Figures 3 and 4 show the nondimensionalized center deflection, $\bar{w} = w/h$, and nondimensionalized center stress, $\bar{\sigma} = \sigma a^2/Eh^2$, as a function of the load parameter, $P = q_0 a^4/Eh^4$ for simply-supported (SS-3) square plate, under uniformly distributed load. Figure 5 shows similar results for clamped (CC-1) square plate under uniformly distributed load. The results are compared with the Ritz solution of Way [65], double Fourier-series solution of Levy [66], the finite-difference solution of Wang [67], the Galerkin solution of Yamaki [68], and the displacement finite-element solution of Kawai and Yoshimura [69]. Finite-element solutions were computed for the five degrees of freedom (NDF = 5), and for three degrees of freedom (NDF = 3); in the latter case, the in-plane displacements were suppressed. Since suppressing the in-plane displacements stiffens the plate, the deflections are smaller and stresses are larger than those obtained by including the in-plane displacements. Solutions of the other investigators were read from the graphs presented in their papers. The

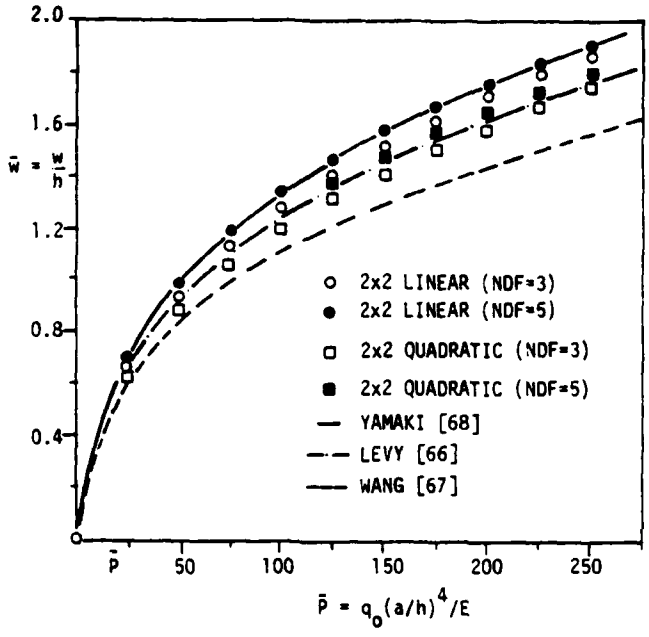

Figure 3. Load-deflection curves by various investigators for simply-supported (SS-3) square plate under uniformly distributed load.

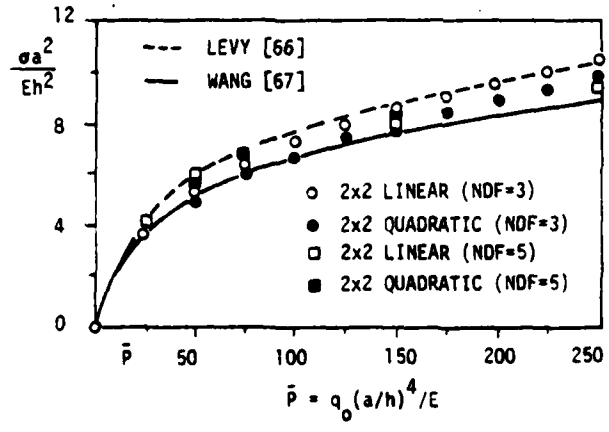

Figure 4. Nondimensionalized center stress versus the load parameter for simply supported (SS-3) square plate under uniformly distributed load.

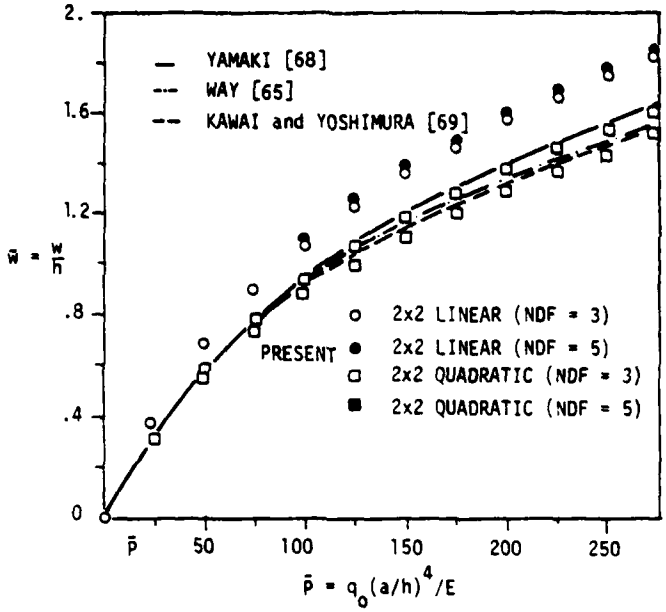

(a) Load-deflection curves

Figure 5. Nondimensionalized center deflection and stress versus the load parameter for clamped (CC-1) square plate under uniformly distributed load.

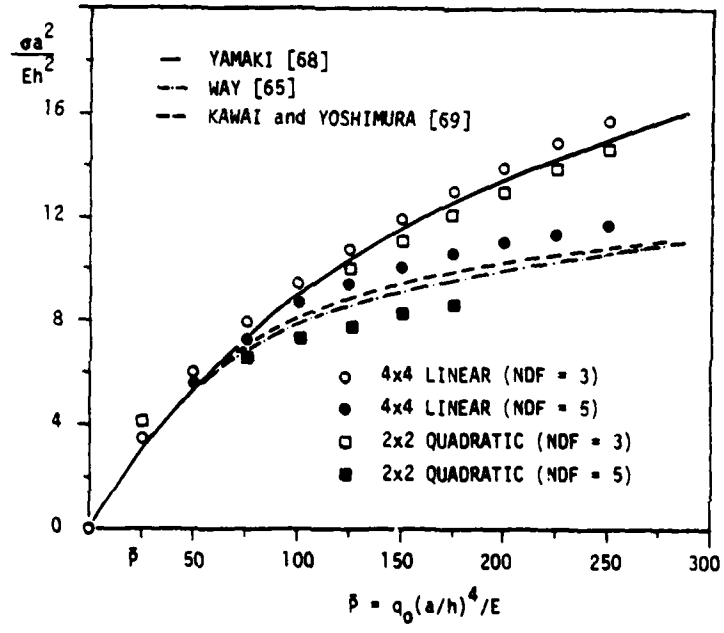

(b) center stress versus load parameter

present solutions are in good agreement with the results of other investigators.

Table 4 Types of boundary conditions used in the present study.

Notation (Type)	Description of essential boundary conditions.	
	side 1	side 2
BC1 (SS-1)	$v = w = \psi_y = 0$	$u = w = \psi_x = 0$
BC2 (SS-2)	$u = w = \psi_y = 0$	$v = w = \psi_x = 0$
BC3 (SS-3)	$u = v = w = 0$	$u = v = w = 0$
BC4 (SS-4)	$u = v = w = \psi_y = 0$	$u = v = w = \psi_x = 0$
BC5 (CC-1)	$u = v = w = \psi_x = 0$	$u = v = w = \psi_y = 0$
BC6 (CC-2)	$u = v = w = \psi_x = \psi_y = 0$	$u = v = w = \psi_x = \psi_y = 0$
BC7 (CC-3)	$u = w = \psi_x = 0$	$v = w = \psi_y = 0$
BC8 (CC-4)	$w = \psi_x = 0$	$w = \psi_y = 0$

Table 5 shows nondimensionalized center deflection $\bar{w} = w_0/h$, center stress $\bar{\sigma}_x^A = \sigma_x^0 a^2/Eh^2$, and edge stress $\bar{\sigma}_x^B = \sigma_x(\frac{a}{2}, 0)a^2/Eh^2$ of a clamped (CC-2) square plate under uniformly distributed load, q_0. The boundary conditions are of type BC6,

CC-2: $u = v = w = \psi_x = \psi_y = 0$ along all edges. (24)

The present solution is obtained using a 2 by 2 uniform mesh (in quarter plate) of nine-node isoparametric elements (2Q9) with (R) and without (F) reduced integration. The present solution for center deflection and stresses agree very closely with the finite element solution of Pica et al. [70], and the analytical solution of Levy [71]. The edge stress, for some reason, does not agree with the other two results.

Table 5 Nondimensionalized center deflection ($\bar{w}$), center stress ($\bar{\sigma}_x^A$), and edge stress ($\bar{\sigma}_x^B$) for clamped (CC-2) square plate under uniformly distributed load (q_o).

$P=\frac{q_o a^4}{Eh^4}$ $\quad \bar{w} = w_o/h$ $\quad \bar{\sigma}_x^A = \sigma_x^A a^2/Eh^2$ $\quad \bar{\sigma}_x^B = \sigma_x^B a^2/Eh^2$

	present (2Q9)		Pica et al.[1]	Levy	present (2Q9)[2]		Pica et al.	Levy	present (2Q9)		Pica et al.	Levy
	F	R	[70]	[71]	F	R	[70]	[71]	F	R	[70]	[71]
17.79	0.1904	0.2455	0.2368	0.237	2.239	2.459	2.6319	2.6	0.8904	0.558	5.3163	5.58
38.3	0.3881	0.4784	0.3699	0.471	4.839	5.129	5.4816	5.2	1.692	1.394	11.216	11.52
63.4	0.5897	0.7045	0.6915	0.695	7.767	7.834	8.3258	8.0	2.373	2.672	17.726	18.03
95.0	0.7909	0.9147	0.9029	0.912	10.97	10.46	11.103	11.1	2.915	4.389	24.967	25.32
134.9	0.9862	1.1189	1.1063	1.121	14.38	13.09	13.827	13.3	3.316	6.606	33.045	33.5
184.0	1.1791	1.3189	1.3009	1.323	17.98	15.75	16.497	15.9	3.568	9.325	41.885	42.4
245.0	1.3781	1.5155	1.4928	1.521	21.89	18.48	19.225	19.2	3.665	12.59	51.719	52.8
318.0	1.5672	1.7020	1.6786	1.714	25.89	21.21	21.994	21.9	3.627	16.29	62.325	63.9
402.0	1.7469	1.8760	1.8555	1.902	29.91	23.89	24.780	25.1	3.464	20.30	73.407	75.8

[1]4Q9 (4 by 4 mesh of 9-node elements).
[2]computed at the nearest Gauss points.

Next, results of large-deflection bending of layered composite plates are presented. First a two-layer ($-\theta°/\theta°$) angle-ply square plate (material II) under uniformly distributed load and simply supported boundary conditions (BC2) was analyzed. Figure 6 shows a plot of nondimensionalized center deflection (w_0/h) and stress $\bar{\sigma} = \sigma_x a^2/E_1 h^2$) versus the orientation (θ) of the layers for the load parameter value ($P = q_0 a^4/E_1 h^4$) of 625. It is interesting to note that the linear deflection and the nonlinear deflection curves do not resemble each other. More specifically, the linear deflection is maximum at $\theta = 15°$ whereas the nonlinear deflection is maximum at $\theta = 45°$. The results were obtained using a 2 by 2 mesh of nine-node element with reduced integration (2Q9).

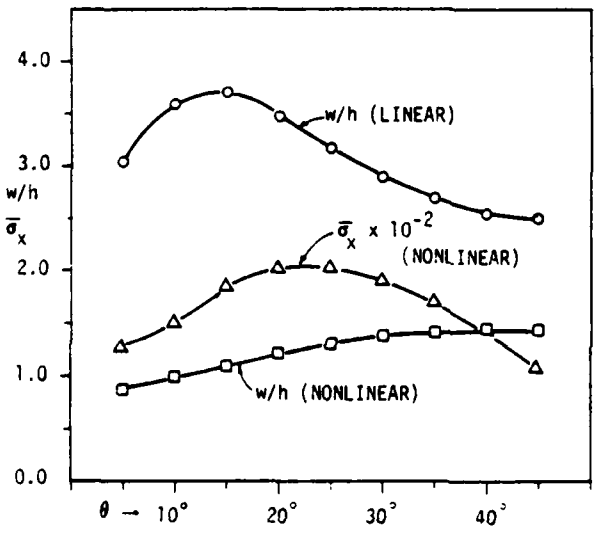

Figure 6. Nondimensionalized center deflection and stress versus the orientation θ for two-layer angle-ply square plate under uniformly distributed loading (material II, a/h = 100, BC2, $\bar{P}$ = 625).

Figure 7 shows nondimensionalized deflection (obtained using 2Q9 mesh) versus the load parameter P for a single-layer (0°) orthotropic (material II) square plate under two loadings (UDL and SSL) and two boundary conditions (BC2 and BC6). The large-deflection results of Chia and Prabhakara [41] cannot be compared with the finite element solution because the boundary conditions used there involve specifying the in-plane stress resultants (N_1, N_2 and N_6). Figure 8 shows the load-deflection curves for four-layer cross-ply and angle-ply square plates (material II, BC6) under uniformly distributed load. The figure also contains, in the case of the angle-ply plate, results for a thick (a/h = 10) plate. For the load parameter value P = 3500, the thick-plate deflection is about 25% higher than the thin-plate deflection; this shows that the shear deformation has significant effect on the deflections

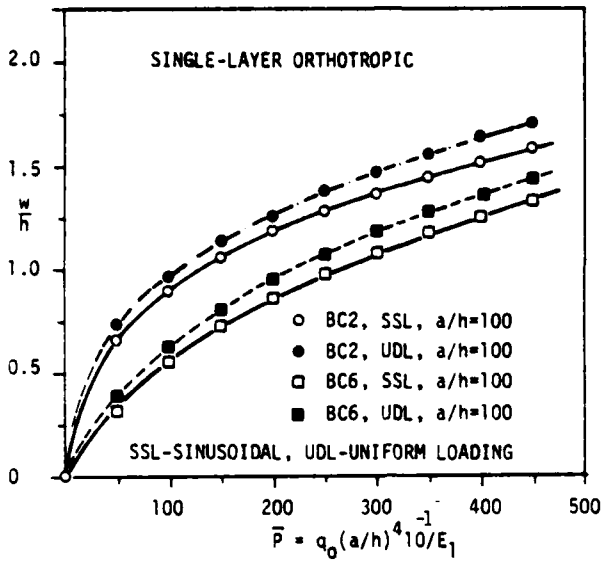

Figure 7. Load-deflection curves for single-layer (0°) orthotropic (material II) plates.

computed. The difference between the thin- and thick-plate deflections increases with the load parameter.

Figure 9 shows the non-dimensionalized deflection versus the load parameter for two-, and six-layer, anti-symmetric (0°/90°/0°/...) cross-ply rectangular plates (material II) subjected to uniform loading. The plate is assumed to be clamped (CC-3), as described in BC7 of Table 4. The present solution (obtained using 2Q8 mesh) is in good agreement, for various aspect ratios, with the perturbation solution of Chia and Prabhakara [41]. Due to lack of tabulated results in [41], the relative differences in the two solutions cannot be discussed.

Figure 10 shows similar results for two-, and six-layer, angle-ply (45°/-45°/-/+...), clamped (CC-2) rectangular plates (material II) subjected to uniform loading. Again, the present result is in close agreement with that of Chia and Prabhakara [41]. The nondimensionalized stress, $\bar{\sigma}_x$, for the cross-ply and angle-ply plates discussed above is plotted against the load parameter in Figure 11.

The effect of the transverse shear strain on the deflection and stresses on the load-deflection, and load-stress curves is shown in Fig. 12. Note that the deflection for a/h = 10 is about 30% larger than that for a/h = 100, at P = 10. That is, the deflections predicted by the classical thin-plate theory are lower than those predicted by the shear deformable theory.

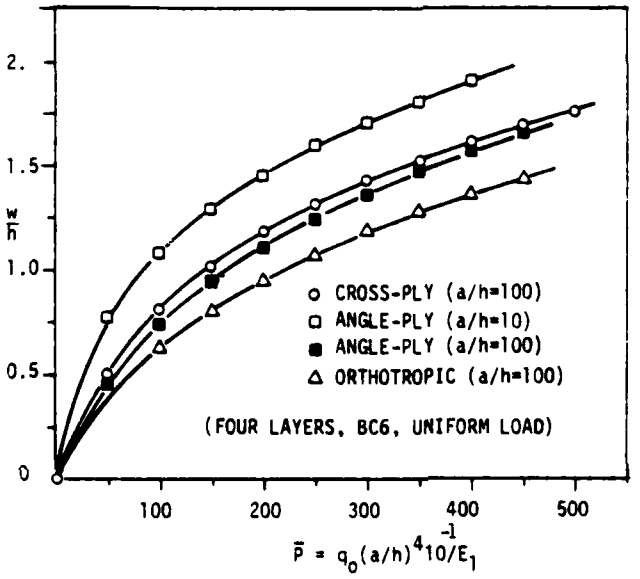

Figure 8. Load-deflection curves for four-layer angle-ply (45°/-45°/45°/-45°) and cross-ply (0°/90°/0°/90°) square plates under uniform loading (material II, BC6).

6.2 Free vibrations results [30-32,44,60].

The effect of reduced integration, and the eight-node element versus the nine-node element were examined for linear frequencies of natural vibration, using a three-layer cross-ply (0°/90°/0°) square plate (material II, BC1). Table 6 shows the nondimensionalized fundamental natural frequency as a function of side-to-thickness ratio, type of integration, and type of element. From the results obtained, it is clear that the reduced integration or mixed (or selective) integration yields relatively better results for all ratios of side-to-thickness ratio.

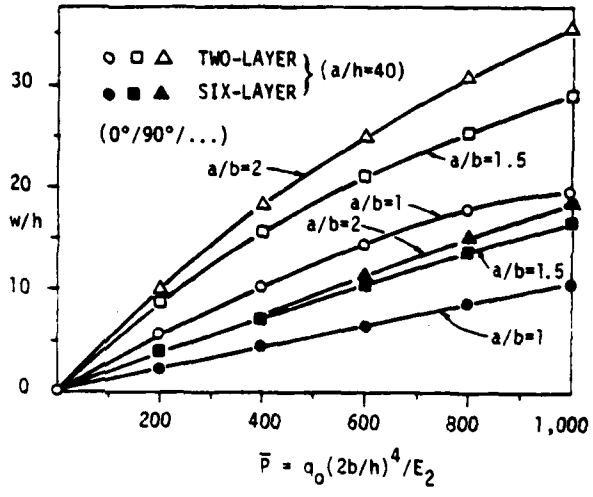

Figure 9. Load-deflection curves for two-layer and six-layer cross-ply (0°/90°/...) rectangular plates (material II, BC7) under uniform loading.

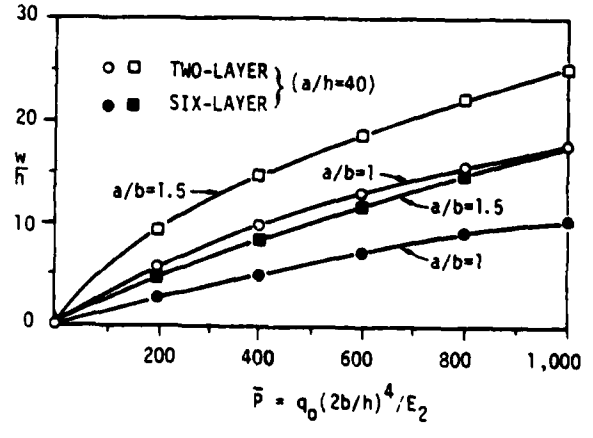

Figure 10. Load-deflection curves for two-layer and six-layer angle-ply (45°/-45°/-+...) rectangular plates (material II, BC7) under uniform loading.

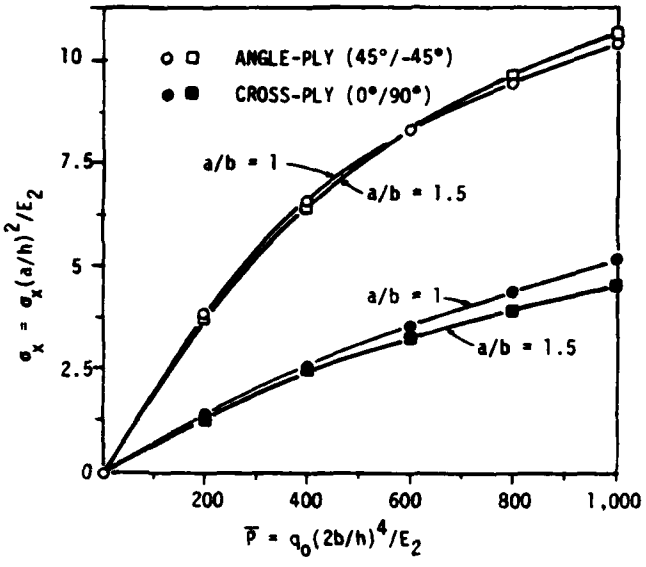

Figure 11. Nondimensionalized center stress versus the load parameter for (a) cross-ply, and (b) angle-ply plates (material II, BC6).

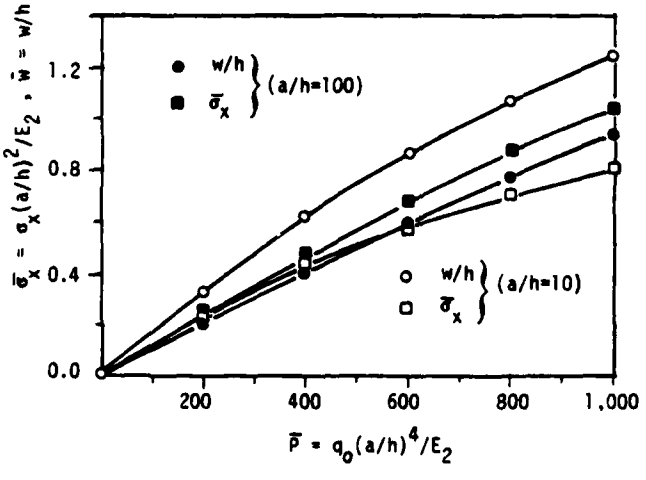

Figure 12. Nondimensionalized center deflection and stress versus the load parameter for four-layer (0°/90°/90°/0°) simply supported (BC1) square plate (material I) under uniform loading.

Table 6 Effects of side-to-thickness ratio, integration, and type of element on the nondimensionalized fundamental frequency = $(\omega a^2/h)\sqrt{P/E_2}$ of a three-layer cross-ply (0°/90°/0°, $h_1 = h_3 = h/4$, $h_2 = h/2$) square plate (material II).

a/h	8-Node Element			9-Node Element			closed-form solution
	R	RF	F	R	RF	F	
2	5.503	5.504	5.502	5.504	--	5.502	5.500
4	9.410	9.397	9.400	9.400	9.394	9.402	9.395
5	10.861	10.857	10.860	10.853	10.867	10.858	10.854
6.25	12.341	12.330	12.340	12.340	12.338	12.339	12.331
10	15.156	15.150	15.161	15.155	15.150	15.159	15.145
12.5	16.201	16.190	16.210	16.201	16.195	16.210	16.189
20	17.677	17.671	17.711	17.676	17.671	17.707	17.665
25	18.089	18.084	18.143	18.088	18.083	18.137	18.093
50	18.698	17.692	18.860	18.693	18.688	18.837	18.675
100	18.874	18.869	19.233	19.855	18.850	19.141	18.733

Figure 13 shows a plot of the nondimensionalized fundamental linear frequency, $\bar{\omega} = \omega a^2/h)\sqrt{\rho/E_2}$, versus the side-to-thickness ratio (a/h) for four-layer cross-ply (0°/90°/90°/0°), and eight-layer angle-ply (45°/45°/+/-...) square plates (material II). The boundary conditions used for the cross-ply plate are those in BC1 and the boundary conditions used for the angle-ply plate are those in BC2. The finite element solutions are compared with the exact closed-form solutions (see Reddy and Chao [31]). The finite element solutions were obtained using a 2 by 2 mesh of eight-node quadratic elements (2Q8). The finite element results agree very closely with the closed-form solutions in both cases.

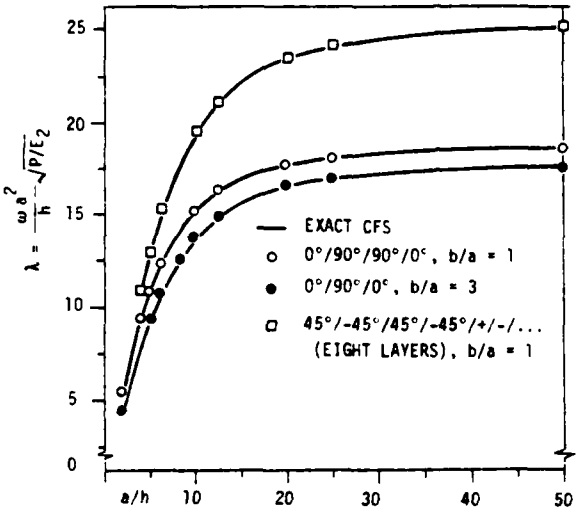

Figure 13. Nondimensionalized fundamental linear frequency versus side-to-thickness ratio for cross-ply (BC1) and angle-ply (BC2) rectangular plates (material II).

To illustrate the accuracy of the present element for nonlinear vibration of plates, linear and nonlinear fundamental frequencies obtained by the present element are compared first with those available in the literature. Table 7 contains ratios of linear to nonlinear fundamental frequencies (ω_L/ω_{NL}) for various amplitude-to-thickness ratios (w_0/h) of simply-supported and clamped square plates ($\nu = 0.3$) as determined by various investigators. Since the other investigators' analyses were based on von Karman plate theory, not including the in-plane displacements, we set b/h = 1000 and suppressed the in-plane degrees of frreedom in the present model. In Ref. [72] a mixed (based on Reissner type functional) finite-element model was employed, while in Refs. [73] and [74] the cubic displacement (based on total potential energy) finite-element model was used. Chu and Herrmann [75] and Yamaki [76] employed Galerkin method to determine the frequencies. The present results were obtained using 2x2 mesh of nine-node quadratic element in the quarter plate, whereas

Table 7 Ratio of linear to nonlinear fundamental frequencies for various amplitude-to-thickness (c/h) ratios of simply-supported and clamped isotropic (ν = 0.3), square plates.

	frequency ratio (ω_L/ω_{NL})				
Source	0.2	0.4	0.6	0.8	1.0
[60] (2x2)	0.9818	0.9331	0.8671	0.7958	0.7271
[72] (4x4)	0.9818	0.9331	0.8670	0.7957	0.7270
[73] (4x4)	0.9818	0.9331	0.8670	0.7958	0.7271
[74] (5x5)	0.9821	0.9338	0.8673	0.7943	0.7233
[75]	0.9809	0.9297	0.8702	0.9853	0.7131
[77]	0.9783	0.9210	0.8451	0.7653	0.6901
[60] (2x2)	0.9929	0.9727	0.9419	0.9038	0.8616
[72] (4x4)	0.9930	0.9730	0.9425	0.9048	0.8631
[73] (4x4)	0.9930	0.9731	0.9427	0.9052	0.8637
[74] (5x5)	0.9930	0.9780	0.9550	0.9320	0.8960
[75]	0.9938	0.9750	0.9460	0.9116	0.8750
[76]	0.9916	0.9716	0.9380	0.8980	0.9566

Table 8 Effect of side-to-thickness ratio (b/h) and edge conditions on nonlinear frequencies of isotropic (ν=0.3) square plates.

Boundary Condition	$\lambda_L \times 10^5$	frequency ratio (ω_L/ω_{NL})[1]				
		0.2	0.4	0.6	0.8	1.0
EC1[2]	0.9499	0.9811	0.9308	0.8630	0.7904	0.7209
EC2[2]	0.9638	0.9818	0.9331	0.8671	0.7958	0.7271
EC3	0.9499	0.9866	0.9494	0.8955	0.8333	0.7692
EC4	0.9638	0.9871	0.9512	0.8990	0.8383	0.7754
EC5	0.9499	0.9992	0.9927	0.9839	0.9720	0.9576
EC1	2332.3	0.9804	0.9285	0.8591	0.7855	0.7155
EC2	2388.0	0.9815	0.9324	0.8658	0.7942	0.7254
EC3	2332.3	0.9862	0.9478	0.8925	0.8290	0.7639
EC4	2388.0	0.9869	0.9506	0.8978	0.8366	0.7733
EC5	2332.3	0.9992	0.9927	0.9838	0.9720	0.9576
EC1	8944.1	0.9788	0.9232	0.8503	0.7745	0.7035
EC2	9308.7	0.9808	0.9300	0.8620	0.7894	0.7203
EC3	8944.1	0.9851	0.9440	0.8854	0.8152	0.8471
EC4	9308.7	0.9864	0.9487	0.8943	0.8315	0.7669

[1]convergence criteria, $\varepsilon = 10^{-3}$

[2]these agree with those of Ref. [70], $\lambda_L = \omega_{11} h\sqrt{\rho/G}$

4x4 mesh of eight-node quadratic element was used in [72]. It is clear that the present resutls are in excellent agreement with the other approximate solutions.

Next the effect of boundary conditions and thickness on the frequency ratio, ω_L/ω_{NL}, is investigated, and the results are shown in Table 8. The boundary (or edge) conditions used in Table 8 are listed in Table 4, and are explained below:

EC1: Three (w,ψ_x,ψ_y)-degree of freedom model, with w specified to be zero on the boundary (i.e., simply-supported edges)-BC3(3DOF)

EC2: same as in BC1, except the tangential rotations are also specified to be zero on the boundary - BC4(3DOF)

EC3: Five (u,v,w,ψ_x,ψ_y)-degree of freedom model with u,v and w specified to be zero on the boundary - BC3.

EC4: Five-degree of freedom model with the transverse deflection, in-plane displacements normal to the boundary, and tangential rotations are specified to be zero at the boundary - BC2.

EC5: Five-degree of freedom model with only the transverse deflection specified to be zero on the boundary.

As can be seen from the results, nonlinear frequencies are more sensitive to the boundary conditions than linear frequencies. This should be expected since the coupling between membrane and flexural stiffnesses is not present in the linear theory. Restraining of the in-plane displacements in effect stiffens the plate and conseuqently, the frequency of vibration increases. Thus, for example, the (nonlinear) frequency of vibration of EC1 (in which u and v are zero everywhere) is larger than that of EC3, although the linear frequencies are identical. In EC5 in-plane displacements are not restrained at all, and therefore thickness has no noticeable effect on the frequency ratio; EC4 is a five-degree of freedom version of EC2.

Figure 14 shows the plot of frequency ratio versus the amplitude-to-thickness ratio for various boundary conditions and side-to-thickness ratio of isotropic ($\nu = 0.3$) square plates. Since the plate stiffness is proportional to the plate thickness, and increases with edge constraints, the nonlinear frequencies are greater for thick plates than for thin plates.

Next, large-deflection free vibration of orthotropic and layered composite plates is discussed. In Table 9, ratios of linear to nonlinear fundamental frequencies are presented for

Table 9 Linear to nonlinear fundamental frequency ratio for various values of the amplitude-to-thickness ratio for single-layer, and two-layer cross-ply square plates under various boundary conditions (material: graphite-epoxy; $\lambda_L = \omega h\sqrt{\rho/E_2}$).

Boundary Condition	amplitude-to-thickness ratio (w_0/h) 0.2	0.4	0.6	0.7	1.0	Linear frequency
EC4 (SL)[1]	0.9792	0.9227	0.8432	0.7555	0.6713	18.819
EC4 (TL-CP)[2]	0.9801	0.9262	0.8510	0.7681	0.6865	16.096
EC5 (TL-CP)	0.9990	0.9912	0.9805	0.9663	0.9490	11.122
EC6 (TL-CP)	0.9990	0.9912	0.9806	0.9664	0.9491	11.173
EC4 (SL)	0.9643	0.8736	0.7611	0.6523	0.5581	14.118
EC4 (TL-CP)	0.9775	0.9174	0.8354	0.7478	0.6649	13.956
EC6 (TL-CP)	0.9976	0.9907	0.9797	0.9651	0.9478	10.300

[1]SL = Single-layer
[2]TL-CP = Two-Layer, Cross-Ply

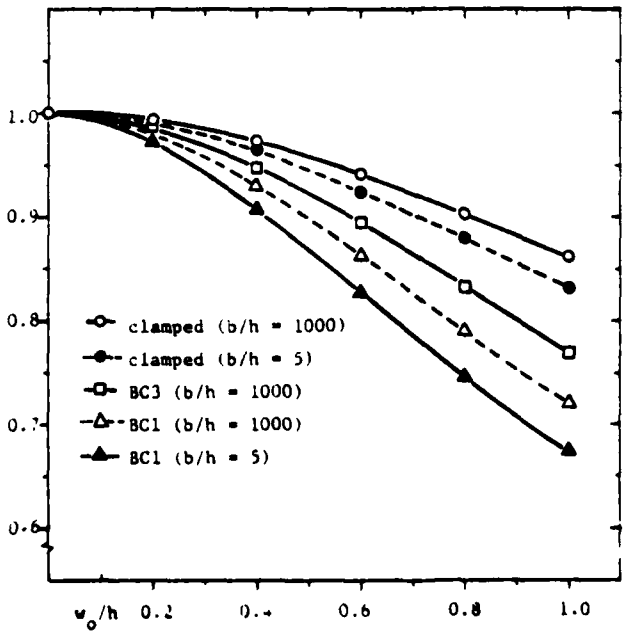

Figure 14. Ratio of linear to nonlinear fundamental frequencies ($\gamma = \omega_L/\omega_{NL}$) versus the amplitude-to-thickness ratio (w_o/h) for isotropic ($\nu = 0.3$) square plates (in-plane degrees of freedom not included).

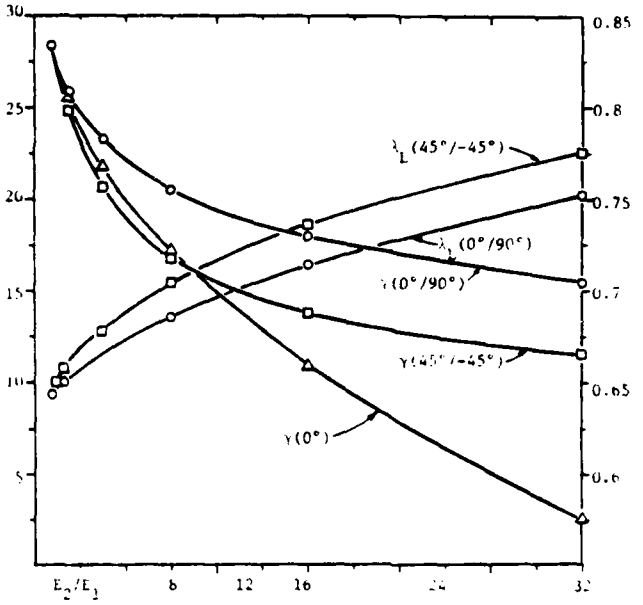

Figure 15. Effect of orthotropy (G_{12}/E_2 = 0.3846, ν_{12} = 0.3) on the linear nondimensionalized fundamental frequency (λ) and on the ratio ($\omega = \omega_L/\omega_{NL}$) of linear to nonlinear fundamental frequencies of square plates (b/h = 10).

single-layer orthotropic and two-layer cross-ply square plates under various boundary conditions. The material properties used are those of graphite-epoxy material ($G_{12} = G_{23} = G_{13}$), material II, and the edge conditions EC6 are described below:

EC6: same as EC4, except no in-plane displacements are specified on the boundary (or same as EC5, except the tangential rotations are also specified on the boundary).

Couple of observations can be made from the results presented in Table 9. First, there is no difference in the frequencies obtained by EC5 and EC6. In other words, specification of the tangential rotations does not alter the vibration frequencies appreciably. As one might suspect, the frequencies obtained by EC4 and EC5 are noticeably different; the nonlinear fundamental frequencies of EC4 are much larger than those of EC5 and EC6. Second, there is a reduction of about 38% in frequencies from single-layer to two-layer (for the same total thickness) plates.

Figure 15 shows the effect of orthotropy (E_1/E_2 for fixed G_{12}/E_2 = 0.3846, ν_{12} = 0.3) on the linear fundamental frequencies and on the ratio of linear to nonlinear frequencies of single-layer and two-layer cross-ply square plates (b/h = 10) subjected to boundary condition EC4. While

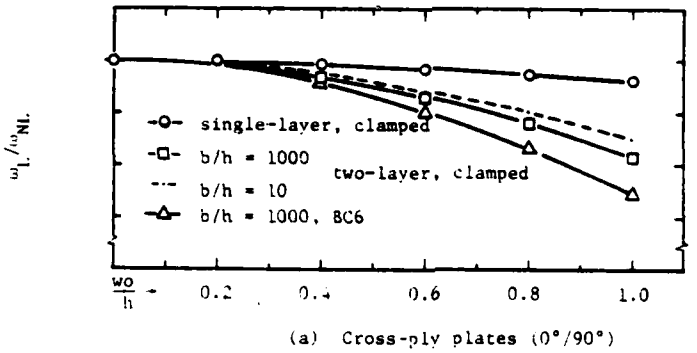

(a) Cross-ply plates (0°/90°)

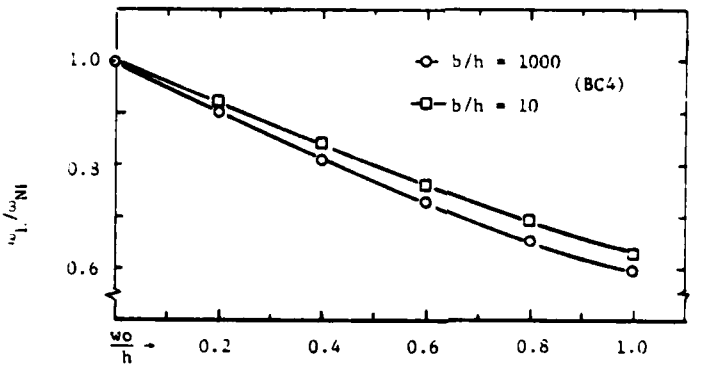

(b) Angle-ply plates (45°/-45°)

Figure 16. Ratio of linear to nonlinear fundamental frequencies versus amplitude to thickness ratio of single-layer and two-layer square plates (E_1/E_2 = 40, G_{12}/E_2 = 0.5, ν_{12} = 0.25).

the linear frequencies increase, the ratio of linear to nonlinear frequencies decreases with increasing E_1/E_2. Although the linear fundamental frequency of the angle-ply plate is larger than the cross-ply plate, the ratio ω_L/ω_{NL} is smaller for angle-ply plate than for the cross-ply plate. This indicates that the nonlinearity is more pronounced in the angle-ply plate than in the cross-ply plate.

Lastly, Figure 16 shows plots of linear to nonlinear frequencies versus the amplitude-to-thickness ratio for two-layer clamped (transverse deflection and the normal rotation are set to zero on the boundary-BC8) square plates of graphite-epoxy material; plots for thin (b/h = 1000) and thick (b/h = 10), cross-ply as well as angle-ply plates are shown in Fig. 16.

7. SUMMARY AND CONCLUSIONS

A finite element based on a shear deformable theory (see [14]) and von Karman (large rotations) theory of layered composite plates is reviewed and numerical results for static bending and free vibrations are presented for isotropic, orthotropic, and layered composite plates of rectangular geometry. It is noted that the nonlinearity is less pronounced in the layered composite plates than in the isotropic plates.

From the study it can be concluded that the four-node and nine-node isoparametric elements (with reduced integration for shear energy terms) give accurate results while possessing simplicity over traditional plate elements. As pointed out earlier (also, see [79-81]), the element can be viewed as one based on a penalty function formulation of classical thin plate theory with the slope continuity conditions as constraints. The penalty terms (i.e., shear energy terms) in the stiffness matrix must be evaluated using reduced integration in order to avoid so-called locking (i.e., to avoid excessively stiff elements; see [82]). An extension of the penalty-function method to enforce the inter-element slope continuity needs further investigation (see Haugeneder [83]). A study of the mathematical properties (e.g., stability, error estimates, etc.) of the plate bending element presented herein is not complete (see, Ohtake, Oden, and Kikuchi [84,85] for some preliminary results).

Although the shear deformable theory of layered composite plates presented here yields acceptable solutions for global response of the plate, locally (i.e., point-wise) the theory does not predict stresses accurately. The questions relating to interlaminar stresses, edge effects, and delamination in composites (see [86-95]) can be addressed only when a higher order, three-dimensional theory is employed (see [96-100]). The comments made above also apply to the case of laminated

composite shells. Thus, developments in computational mechanics related to finite-element analysis of plates and shells in the next decade would largely concern with the development of computationally simple elements that are capable of representing accurately physical features of the phenomena involved.

ACKNOWLEDGMENTS

The results presented in the paper were obtained during investigations supported by Structures Mechanics Programs of the Office of Naval Research (N00014-78-C-0647), and the Air Force Office of Scientific Research (Grant AFSOR-81-0142). The support is gratefully acknowledged. It is also a pleasure to acknowledge the skillful typing of the manuscript by Mrs. Vanessa McCoy.

REERENCES

1. STAVSKY, Y. - On the Theory of Symmetrically Heterogeneous Plates Having the Same Thickness Variation of the Elastic Moduli. Topics in Applied Mechanics, Ed. Abir, D., Ollendorff, F. and Reiner, M., American Elsevier, New York, 1965.

2. YANG, P. C., NORRIS, C. H. and STAVSKY, Y. - Elastic Wave Propagation in Heterogeneous Plates. Int. J. Solids and Structures, Vol. 2, pp. 665-684, 1966.

3. SUN, C. T. and WHITNEY, J. M. - Theories for the Dynamic Response of Laminated Plates. AIAA J., Vol. 11, pp. 178-183, 1973.

4. WHITNEY, J. M. and SUN, C. T. - A Higher Order Theory for Extensional Motion of Laminated Composites. J. Sound and Vibration, Vol. 30, pp. 85-97, 1973.

5. SRINIVAS, S. and RAO, A. K. - Bending, Vibration and Buckling of Simply Supported Thick Orthotropic Rectangular Plates and Laminates. Int. J. Solids and Structures, Vol. 6, pp. 1463-1481, 1970.

6. SRINIVAS, S., JOGA RAO, C. V. and RAO, A. K. - An Exact Analysis for Vibration of Simply Supported Homogeneous and Laminated Thick Rectangular Plates, J. Sound and Vibration, Vol. 12, pp. 187-199, 1970.

7. HUSSAINY, S. A. and SRINIVAS, S. - Flexure of Rectangular Composite Plates. Fibre Science and Technology, Vol. 8, pp. 59-76, 1975.

8. BERT, C. W. - Analysis of Plates. Structural Design and Analysis, Part I, Ed. Chamis, C. C., Academic Press, New York, 1974.

9. PAGANO, N. J. - Exact Solutions for Composite Laminates in Cylindrical Bending. J. of Composite Materials, Vol. 3, No. 3, pp. 398-411, 1969.

10. PAGANO, N. J. - Exact Solutions for Rectangular Bidirectional Composites and Sandwich Plates. J. of Composite Materials, Vol. 4, pp. 20-34, 1970.

11. PAGANO, N. J. and HATFIELD, S. J. - Elastic Behavior of Multilayer Bidirectional Composites. AIAA Journal, Vol. 10, pp. 931-933, 1972.

12. WHITNEY, J. M. - The Effect of Transverse Shear Deformation on the Bending of Laminated Plates. J. Composite Materials, Vol. 3, No. 3, pp. 534-547, 1969.

13. MAU, S. T. - A Refined Laminated Plate Theory. J. Appl. Mech., Vol. 40, pp. 606-607, 1973.

14. WHITNEY, J. M. and PAGANO, N. J. - Shear Deformation in Heterogeneous Anisotropic Plates. J. Appl. Mech., Vol. 37, pp. 1031-1036, 1970.

15. FORTIER, R. C. and ROSSETTOS, J. N. - On the Vibration of Shear Deformable Curved Anisotropic Composite Plates. J. Appl. Mech., Vol. 40, pp. 299-301, 1973.

16. SINHA, P. K. and RATH, A. K. - Vibration and Buckling of Cross-Ply Laminated Circular Cylindrical Panels. Aeronautical Quarterly, Vol. 26, pp. 211-218, 1975.

17. BERT, C. W. and CHEN, T. L. C. - Effect of Shear Deformation on Vibration of Antisymmetric Angle-Ply Laminated Rectangular Plates. Int. J. Solids and Structures, Vol. 14, pp. 465-473, 1978.

18. PRYOR, JR., C. W. and BARKER, R. M. - A Finite Element Analysis Including Transverse Shear Effects for Applications to Laminated Plates. AIAA J., Vol. 9, pp. 912-917, 1971.

19. BARKER, R. M., LIN. F. T. and DANA, J. R. - Three-Dimensional Finite-Element Analysis of Laminated Composites. National Symposium on Computerized Structural Analysis and Design, George Washington University, 1972.

20. MAU, S. T., TONG, P. and PIAN, T. H. H. - Finite Element Solutions for Laminated Thick Plates. J. Composite Materials, Vol. 6, pp. 304-311, 1972.

21. MAU, S. T. and WITMER, E. A. - Static, Vibration, and Thermal Stress Analyses of Laminated Plates and Shells by the Hybrid-Stress Finite Element Method with Transverse Shear Deformation Effects Included. Aeroelastic and Structures Research Laboratory, Report ASRL TR 169-2, Department of Aeronautics and Astronautics, MIT, Cambridge, MA, 1972.

22. NOOR, A. K. and MATHERS, M. D. - Anisotropy and Shear Deformation in Laminated Composite Plates. AIAA J., Vol. 14, pp. 282-285, 1976.

23. NOOR, A. K. and MATHERS, M. D. - Finite Element Analysis of Anisotropic Plates. Int. J. Num. Meth. Engng., Vol. 11, pp. 289-307, 1977.

24. HINTON, E. - A Note on a Thick Finite Strip Method for the Free Vibration of Laminated Plates. Earthquake Eng. and Struct. Dynamics., Vol. 4, pp. 511-514, 1976.

25. HINTON, E. - Flexure of Composite Laminates Using the Thick Finite Strip Method. Computers and Structures, Vol. 7, pp. 217-220, 1977.

26. MAWENYA, A. S. and DAVIES, J. D. - Finite Element Bendin Analysis of Multilayer Plates. Int. J. Num. Meth. Engng., Vol. 8, pp. 215-225, 1974.

27. PANDA, S. C. and NATARAJAN, R. - Finite Element Analysis of Laminated Composite Plates. Int. J. Num. Meth. Engng., Vol. 14, pp. 69-79, 1979.

28. AHMAD, S., IRONS, B. M. and ZIENKIEWICZ, O. C. - Analysis of Thick and Thin Shell Structures by Curved Finite Elements. Int. J. Num. Meth. Engng., Vol. 2, pp. 419-451, 1970.

29. SPILKER, R. L., CHOU, S. C. and ORRINGER, O. - Alternate Hybrid Stress Elements for Anslysis of Multilayer Composite Plates. J. Composite Materials, Vol. 11, pp. 51-70, 1977.

30. REDDY, J. N. - A Penalty Plate-Bending Element for the Analysis of Laminated Anisotropic Composite Plates. Int. J. Numer. Meth. Engng., Vol. 15, pp. 1187-1206, 1980.

31. REDDY, J. N. and CHAO, W. C. - A Comparison of Closed-Form and Finite Element Solutions of Thick Laminated Anisotropic Rectangular Plates. Nuclear Engineering and Design, Vol. 64, 1981, to appear.

32. REDDY, J. N. - Free Vibration of Antisymmetric, Angle-Ply Laminated Plates, Including Transverse Shear Deformation by the Finite Element Method. J. Sound and Vibration, Vol. 66, No. 4, pp. 565-576, 1979.

33. REDDY, J. N. and BERT, C. W. - Analyses of Plates Constructed of Fiber-Reinforced Bimodulus Materials. Mechanics of Bimodulus Materials, Ed. Bert, C. W., AMD Vol. 33, American Society of Mechanical Engineers, New York, pp. 29-37, 1979.

34. REDDY, J. N. and CHAO, W. C. - Finite-element Analysis of Laminated Bimodulus Composite-Material Plates. Computers and Structures, Vol. 12, pp. 245-251, 1980.

35. WHITNEY, J. M. and LEISSA, A. W. - Analysis of Heterogeneous Anisotropic Plates. J. Appl. Mech., Vol. 36, pp. 261-266, 1969.

36. BENNETT, J. A. - Nonlinear Vibration of Simply Supported Angle Ply Laminated Plates. AIAA J., Vol. 9, pp. 1997-2003, 1971.

37. BERT, C. W. - Nonlinear Vibration of a Rectangular Plate Arbitrarily Laminated of Anisotropic Material. J. Appl. Mech., Vol. 40, pp. 452-458, 1973.

38. CHANDRA, R. and RAJU, B. B. - Large Amplitude Flexural Vibration of Cross Ply Laminated Composite Plates. Fibre Science and Technology, Vol. 8, pp. 243-263, 1975.

39. CHANDRA, R. - Large Deflection Vibration of Cross-Ply Laminated Plates with Certain Edge Conditions. J. Sound and Vibration, Vol. 47, No. 4, pp. 509-514, 1976.

40. ZAGHLOUL, S. A. and KENNEDY, J. B. - Nonlinear Analysis of Unsymmetrically Laminated Plates. J. Engng. Mech. Div., ASCE, Vol. 101 (EM3), pp. 169-185, 1975.

41. CHIA, C. Y. and PRABHAKARA, M. K. - Large Deflection of Unsymmetric Cross-Ply and Angle-Ply Plates. J. Mech. Engng. Sci., Vol. 18, No. 4, pp. 179-183, 1976.

42. CHIA, C. Y. and PRABHAKARA, M. K., - A General Mode Approach to Nonlinear Flexural Vibrations of Laminated Rectangular Plates. J. Appl. Mech., Vol. 45, pp. 623-628, 1978.

43. NOOR, A. K. and HARTLEY, S. J. - Effect of Shear Deformation and Anisotropy on the Non-Linear Response of Composite Plates. Developments in Composite Materials - 1, Ed. Holister, G., Applied Science Publishers, Barking, Essex, England, pp. 55-65, 1977.

44. REDDY, J. N. and CHAO, W. C. - Large Deflection and Large Amplitude Free Vibrations of Laminated Composite Material Plates. Computed Structures, Vol. 13, No. 2, pp. 341-347, 1981.

45. REDDY, J. N. and CHAO, W. C. - Non-Linear Bending of Thick Rectangular, Laminated Composite Plates. Int. J. Non-Linear Mechanics, 1981, to appear.

46. AMBARTSUMYAN, S. A. - Theory of Anisotropic Plates (English Translation), Technomic, Stamford, Conn., 1970.

47. HASSERT, J. E. and NOWINSKI, J. L. - Nonlinear Transverse Vibration of a Flat Rectangular Orthotropic Plate Supported by Stiff Rig. Proc. of 5th International Symposium on Space Technology and Science, Tokyo, pp. 561-570, 1962.

48. NOWINSKI, J. L. - Nonlinear Vibrations of Elastic Circular Plates Exhibiting Rectilinear Orthotropy. Zeitschrift fur Angew Methematik and Physik, Vol. 14, pp. 112-124, 1963.

49. NOWINSKI, J. L. and ISMAIL, I. A. - Large Oscillations of an Anisotropic Triangular Plate. J. of the Franklin Institute, Vol. 280, pp. 417-424, 1965.

50. WU, C. I. and VINSON, J. R. - On the Nonlinear Oscillations of Plates Composed of Composite Materials. J. of Composite Materials, Vol. 3, pp. 548-561, 1969.

51. MAYBERRY, B. L. and BERT, C. W. - Experimental Investigation of Nonlinear Vibrations of Laminated Anisotropic Panels. Shock and Vibration Bulletin, Vol. 39, Part 3, pp. 191-199, 1969.

52. NOWINSKI, J. L. - Nonlinear Oscillations of Anisotropic Plates Under Large Initial Stress. Proc. of the 10th Congress of Theoretical and Applied Mechanics, Madras, India, pp. 13-30, 1965.

53. SATHYAMOORTHY, M. and PANDALAI, K. A. - Nonlinear Flexural Vibrations of Orthotropic Rectangular Plates. J. of Aeronautical Society of India, Vol. 22, pp. 264-266, 1970.

54. PRABHAKARA, M. K. and CHIA, C. Y. - Nonlinear Flexural Vibrations of Orthotropic Rectangular Plates. J. of Sound and Vibration, Vol. 52, pp. 511-518, 1977.

55. SATHYAMOORTHY, M. and CHIA, C. Y. - Non-Linear Vibration of Anisotropic Rectangular Plates Including Shear and Rotatory Inertia. Fibre Science and Technology, Vol. 13, pp. 337-361, 1980.

56. SATHYAMOORTHY, M. and CHIA, C. Y. - Effect of Transverse Shear and Rotatory Inertia on Large Amplitude Vibration of Anisotropic Skew Plates, Part 1 - Theory. J. Appl. Mech., Vol. 47, pp. 128-132, 1980.

57. SATHYAMOORTHY, M. and CHIA, C. Y. - Effect of Transverse Shear and Rotatory Inertia on Large Amplitude Vibration of Anisotropic Skew Plates, Part 2 - Numerical Results. J. Appl. Mech., Vol. 47, pp. 133-138, 1980.

58. WU, C. I. and VINSON, J. R. - Nonlinear Oscillations of Laminated Specially Orthotropic Plates with Clamped and Simply Supported Edges. Journal of the Acoustical Society of America, Vol. 49, pp. 1561-1567, 1971.

59. CHANDRA, R. and BASAVA RAJU, B. - Large Deflection Vibration of Angle Ply Laminated Plates. Journal of Sound and Vibration, Vol. 40, pp. 393-408, 1975.

60. REDDY, J. N. - Nonlinear Vibration of Layered Composite Plates Including Transverse Shear and Rotatory Inertia. 1981 ASME Vibration Conference, Hartford, Connecticut, September 20-23, 1981.

61. REDDY, J. N. - Simple Finite Elements with Relaxed Continuity for Nonlinear Analysis of Plates. Proc. Third Int. Conf. in Australia on Finite Element Methods, University of New South Wales, Sydney, July 2-6, 1979.

62. ZIENKIEWICZ, O. C., TAYLOR, R. L. and TOO, J. M. - Reduced Integration Technique in General Analysis of Plates and Shells. Int. J. Num. Meth. Engng., Vol. 3, pp. 575-586, 1971.

63. HUGHES, T. J. R., COHEN, M. and HAROUN, M. - Reduced and Selective Integration Techniques in the Finite Element Analysis of Plates. Nuclear Engineering and Design, Vol. 46, pp. 203-222, 1978.

64. WHITNEY, J. M. - Stress Analysis of Thick Laminated Composite and Sandwich Plates. J. Composite Materials, Vol. 6, pp. 426-440, 1972.

65. WAY, S. - Uniformly Loaded, Clamped, Rectangular Plates with Large Deformation. Proc. 5th Int. Congr. Appl. Mech. (Cambridge, Mass., 1938), John Wiley, pp. 123-238, 1939.

66. LEVY, S. - Bending of Rectangular Plates with Large Deflections. Report No. 737, NACA, 1942.

67. WANG, C. T. - Bending of Rectangular Plates with Large Deflections. Report No. 1462, NACA, 1948.

68. YAMAKI, N. - Influence of Large Amplitudes on Flexural Vibrations of Elastic Plates. ZAMM, Vol. 41, pp. 501-510, 1967.

69. KAWAI, T. and YOSHIMURA, N. - Analysis of Large Deflection of Plates by the Finite Element Method. Int. J. Numer. Meth. Engng., Vol. 1, pp. 123-133, 1969.

70. PICA, A., WOOD, R. D. and HINTON, E. - Finite Element Analysis of Geometrically Nonlinear Plate Behavior Using a Mindlin Formulation. Computers & Structures, Vol. 11, pp. 203-215, 1980.

71. LEVY, S. - Square Plate with Clamped Edges Under Pressure Producing Large Deflections. NACA, Tech. Note 847, 1942.

72. REDDY, J. N. and STRICKLIN, J. D. - Large Deflection and Large Amplitude Free Vibrations of Thin Rectangular Plates Using Mixed Isoparametric Elements. Applications of Computer Methods in Engineering, Vol. II, Ed. Wellford, Jr., L. C., University of Southern California, Los Angeles, pp. 1323-1335, 1977.

73. RAO, G. V., RAJU, I. S., KANAKA RAJU, K. - A Finite Element Formulation for Large Amplitude Flexural Vibrations of Thin Rectangular Plates. Computers & Structures, Vol. 6, pp. 163-167, 1976.

74. MEI, C. - Finite Element Displacement Method for Large Amplitude Free Flexural Vibrations of Beams and Plates. Computers & Structures, Vol. 3, pp. 163-174, 1973.

75. CHU, H. N. and HERRMANN, G. - Influence of Large Amplitudes on Free Flexural Vibrations of Rectangular Elastic Plates. J. of Applied Mechanics, Vol. 23, pp. 532-540, 1956.

76. YAMAKI, N. - Influence of Large Amplitudes on Flexural Vibrations of Elastic Plates. ZAMM, Vol. 41, pp. 501-510, 1967.

77. WAH, T. - Large Amplitude Flexural Vibration of Rectanqular Plates. Int. J. Mech. Sci., Vol. 5, pp. 425-438, 1963.

78. KANAKA RAJU, K. and HINTON, E. - Nonlinear Vibrations of Thick Plates Usinq Mindlin Plate Elements. Int. J. Numer. Meth. Engng., Vol. 15, pp. 249-257, 1980.

79. WESTBROOK, D. R., CHAKRABARTI, S. and CHEUNG, Y. K. - A Three-Dimensional Finite Element Method for Plate Bending. Int. J. Mech. Sci., Vol. 16, pp. 479-487, 1974.

80. WESTBROOK, D. R., CHAKRABARTI, S. and CHEUNG, Y. K. - A Three-Dimensional or Penalty Finite Element Method for Plate Bending. Int. J. Mech. Sci., Vol. 18, pp. 347-350, 1976.

81. HUGHES, T. J. R., TAYLOR, R. L. and KANOKNUKULCHAI, W. - A Simple and Efficient Finite Element for Plate Bending. Int. J. Numer. Meth. Engng., Vol. 11, pp. 1529-1543, 1977.

82. ZIENKIEWICZ, O. C. and HINTON, E. - Reduced Integration, Function Smoothing and Non-Conformity in Finite Element Analysis. J. Franklin Inst., Vol. 302, pp. 443-461, 1976.

83. HAUGENEDER, E. - A New Penalty Function Element for Thin Shell Analysis. Seventeenth Annual Meeting of the Society of Engineering Science, Georgia Institute of Technology, Atlanta, GA, December 15-17, 1980.

84. OHTAKE, O., ODEN, J. T. and KIKUCHI, N. - Analysis of Certain Unilateral Problems in von Karman Plate Theory by a Penalty Method - Part 1. A Variational Principle with Penalty. Comp. Meth. in Appl. Mech. Engng., Vol. 24, pp. 187-213, 1980.

85. OHTAKE, O., ODEN, J. T. and KIKUCHI, N. - Analysis of Certain Unilateral Problems in von Karman Plate Theory by a Penalty Method - Part 2. Approximation and Numerical Analysis. Comp. Meth. in Appl. Mech. Engng., Vol. 24, pp. 317-337, 1980.

86. HAYASHI, T. - Analytical Study of Interlaminar Shear Stresses in a Laminated Composite Plate. Trans. Japan Soc. Aero. Engng. Space Sciences, Vol. 10, No. 47, p. 43, 1967.

87. PAGANO, N. J. - Stress Fields in Composite Laminates. Int. J. Solids Structures, Vol. 14, pp. 385-400, 1978.

88. PAGANO, N. J. - Free Edge Stress Fields in Composite Laminates. Int. J. Solids Structures, Vol. 14, pp. 401-406, 1978.

89. WANG, A. S. D. and CROSSMAN, F. W. - Some New Results on Edge Effect in Symmetric Composite Laminates. J. Composite Materials, Vol. 8, pp. 92-106, 1977.

90. SALAMON, N. J. - Interlaminar Stresses in a Layered Composite Laminate in Bending. Fibre Science and Technology, Vol. 11, pp. 305-317, 1978.

91. WANG, S. S. and CHOI, I. - Boundary Layer Thermal Stresses in Angle-Ply Composite Laminates. Modern Developments in Composite Materials and Structures, Ed. Vinson, J. R., American Society of Mechanical Engineers, New York, pp. 315-341, 1979.

92. WANG, S. S. - Edge Delamination in Angle-Ply Composite Laminates. Proc. 22nd AIAA/ASME/SAE Structures, Structural Dynamics, and Materials Conference, Atlanta, GA, pp. 473-484, 1981.

93. SPILKER, R. L. and CHOU, S. C. - Edge Effects in Symmetric Composite Laminates: Importance of Satisfying the Traction-Free-Edge Condition. J. Composite Materials, Vol. 14, pp. 2-20, 1980.

94. RAJU, I. S. and CREWS, Jr., J. H. - Interlaminar Stress Singularities at a Straight Free Edge in Composite Laminates. NASA Technical Memorandum 81876, Langley Research Center, Hampton, VA, 1980.

95. RAJU, I. S., WHITCOMB, J. D. and GOREE, J. G. - A New Look at Numerical Analyses of Free-Edge Stresses in Composite Laminates. NASA Technical Paper 1751, Langley Research Center, Hampton, VA 1980.

96. WHITNEY, J. M. and SUN, C. T. - A Refined Theory for Laminated Anisotropic, Cylindrical Shells. J. Appl. Mech., Vol. , pp. 471-476, 1974.

97. LO, K. H., CHRISTENSEN, R. M. and WU, E. M. - A Higher-Order Theory of Plate Deformation, Part 1: Homogeneous Plates. J. Appl. Mech., Vol. 44, pp. 662-668, 1977.

98. LO, K. H., CHRISTENSEN, R. M. and WU, E. M. - A Higher-Order Theory of Plate Deformation, Part 2: Laminated Plates. J. Appl. Mech., Vol. 44, pp. 669-676, 1977.

99. SPILKER, R. L. - Higher Order Three-Dimensional Hybrid-Stress Elements for Thick-Plate Analyses. Int. J. Numer. Meth. Engng, Vol. 17, pp. 53-69, 1981.

100. ALTUS, E., ROTEM, A. and SHMUELI, M. - Free Edge Effect in Angle Ply Laminates - A New Three Dimensional Finite Difference Solution. J. Composite Materials, Vol. 14, pp. 21-30, 1980.

APPENDIX A: NOMENCLATURE

A_{ij}, B_{ij}, D_{ij}	extensional, flexural-extensional and flexural stiffnesses (i,j = 1,2,6).
a,b	plate planform dimensions in x,y directions, respectively
E_1, E_2	layer elastic moduli in directions along fibers and normal to them, respectively
C_n, C_m, C_q	boundary segments of domain R
G_{12}, G_{13}, G_{23}	layer in-plane and thickness shear moduli
h, h_i	total thickness of the plate; thickness of i-th layer
I	rotatory inertia coefficient per unit midplane area of lamina
k_i	shear correction coefficients associated with the yz and xz planes, respectively (i = 1,2)
$K_{ij}^{\alpha\beta}$	element stiffness coefficients (α, β = 1,2,...,5; i,j = 1,2,...,n)
L	total number of layers in the plate
M_i, N_i	stress couple and stress resultant, respectively (i = 1,2,6)
$M_{ij}^{\alpha\beta}$	element mass coefficients (α, β = 1,2,...,5; i,j = 1,2,...,n)
n	number of nodes per element
P	laminate normal inertia coefficient per unit midplane area
Q_i	shear stress resultant (i = 1,2)
Q_{ij}	plane-stress reduced stiffness coefficients (i,j = 1,2,6)

q_o	intensity of transversely distributed load
R	laminate rotatory-normal coupling inertia coefficient per unit midplane area
$\mathbb{R}$; $\mathbb{R}_e$	domain (midplane of the plate); typical element
$R_{ij}^{\xi\eta\xi}, S_{ij}^{\xi\eta}$	element matrices in FEM formulation (ξ,η,ζ = 0, x,y; i,j = 1,2,...,n)
t	time
u_1,u_2,u_3	displacement components in x,y,z directions, respectively
u,v	in-plane displacements in x,y directions
U,U_i, etc.	typical variable and its nodal value, respectively
x,y,z	position coordinates in cartesian system
$\{\Delta\}$	column of vector of generalized nodal displacements
ε_i	strain components (i = 1,2,...,6)
θ_m	orientation of m-th layer (m = 1,2,...,L)
$\rho(m)$	density of m-th layer (m = 1,2,...,L)
λ	nondimensional fundamental frequency
σ_i	stress components (i = 1,2,...,6)
ϕ_i	finite-element interpolation functions (i = 1,2,...,n)
ψ_x,ψ_y	bending slope (rotation) functions
κ_i	plate curvatures (i = 1,2,6)
ω	fundamental frequency of free vibration (ω_L = linear; ω_{NL} = nonlinear)

APPENDIX B: ELEMENTS OF STIFFNESS AND MASS MATRICES

stiffness matrix:

$$[K] = \begin{bmatrix} \tau[K^{11}] & \tau[K^{12}] & \lambda^2[K^{13}] & \mu[K^{14}] & \mu[K^{15}] \\ \tau[K^{21}] & \tau[K^{22}] & \lambda^2[K^{23}] & \mu[K^{24}] & \mu[K^{25}] \\ \lambda\tau[K^{31}] & \lambda\tau[K^{32}] & \lambda[K_1^{33}] & \mu[K_1^{34}] & \mu[K_1^{35}] \\ & & +\lambda^3[K_2^{33}] & +\mu\lambda[K_2^{34}] & +\mu\lambda[K_2^{35}] \\ \tau[K^{41}] & \tau[K^{42}] & \lambda[K_1^{43}] & \mu[K^{44}] & \mu[K^{45}] \\ & & +\lambda^2[K_2^{43}] & & \\ \tau[K^{51}] & \tau[K^{52}] & \lambda[K_1^{53}] & \mu[K^{54}] & \mu[K^{55}] \\ & & +\lambda^2[K_2^{53}] & & \end{bmatrix}$$

mass matrix:

$$[M] = \begin{bmatrix} P[S] & [0] & [0] & R[S] & [0] \\ [0] & P[S] & [0] & [0] & R[S] \\ [0] & [0] & P[S] & [0] & [0] \\ R[S] & [0] & [0] & I[S] & [0] \\ [0] & R[S] & [0] & [0] & I[S] \end{bmatrix}$$

The matrix coefficients $K_{ij}^{\alpha\beta}$ are given by

$$[K^{11}] = A_{11}[S^{xx}] + A_{16}([S^{xy}] + [S^{xy}]^T) + A_{66}[S^{yy}],$$

$$[K^{12}] = A_{12}[S^{xy}] + A_{16}[S^{xx}] + A_{26}[S^{yy}] + A_{66}[S^{xy}]^T = [K^{21}]^T,$$

$$[K^{13}] = A_{11}[R_x^{xx}] + A_{12}[R_y^{xy}] + A_{16}([R_x^{xy}] + [R_x^{xy}]^T + [R_y^{xx}])$$

$$+ A_{26}[R_y^{yy}] + A_{66}([R_y^{xy}]^T + [R_x^{yy}]) = \frac{1}{2}[K^{31}]^T,$$

$$[K^{14}] = B_{11}[S^{xx}] + B_{16}([S^{xy}] + [S^{xy}]^T) + B_{66}[S^{yy}] = [K^{41}]^T,$$

$$[K^{15}] = B_{12}[S^{xy}] + B_{16}([S^{xy}] + B_{26}[S^{yy}] + B_{66}[S^{xy}]^T = [K^{51}]^T$$

$$[K^{22}] = A_{22}[S^{yy}] + A_{26}([S^{xy}]^T + [S^{xy}]) + A_{66}[S^{xx}],$$

$$[K^{23}] = A_{12}[R_x^{xy}]^T + A_{22}[R_y^{yy}] + A_{26}([R_y^{xy}]^T + [R_y^{xy}] + [R_x^{y}])$$

$$+ A_{16}[R_x^{xx}] + A_{66}([R_x^{xy}] + [R_y^{xx}]) = \frac{1}{2}[K^{32}]$$

$$[K^{24}] = B_{12}[S^{xy}]^T + B_{26}[S^{yy}] + B_{16}[S^{xx}] + B_{66}[S^{xy}]$$

$$= [K^{42}]^T,$$

$$[K^{25}] = B_{22}[S^{yy}] + B_{26}([S^{xy}] + [S^{xy}]^T) +$$

$$B_{66}[S^{xx}] = [K^{52}]^T$$

$$[K_1^{33}] = A_{55}[S^{xx}] + A_{45}([S^{xy}] + [S^{xy}]^T) + A_{44}[S^{yy}],$$

$$[K_2^{33}] = \frac{1}{2}\int_{R^e}[\bar{N}_1 \frac{\partial\phi_i}{\partial x}\frac{\partial\phi_j}{\partial x} + \bar{N}_6 (\frac{\partial\phi_i}{\partial x}\frac{\partial\phi_j}{\partial x}) +$$

$$\bar{N}_2 \frac{\partial\phi_i}{\partial y}\frac{\partial\phi_j}{\partial y}]dxdy,$$

$$[K_1^{34}] = A_{55}[S^{xo}] + A_{45}[S^{yo}] = [K_1^{43}]^T,$$

$$[K_2^{34}] = B_{11}[R_x^{xx}] + B_{16}([R_x^{xy}] + [R_x^{xy}]^T + [R_y^{xx}])$$

$$+ B_{12}[R_y^{xy}]^T + B_{26}[R_y^{yy}] + B_{66}([R_x^{yy}] + [R_y^{xy}])$$

$$= 2[K_2^{43}]^T,$$

$$[K_1^{35}] = A_{45}[S^{xo}] + A_{44}[S^{yo}] = [K_1^{53}]^T,$$

$$[K_2^{35}] = B_{12}[R_x^{xy}] + B_{16}[R_x^{xx}] + B_{22}[R_y^{yy}] + B_{26}([R_y^{xy}]^T +$$

$$[R_x^{yy}] + [R_y^{xy}]) + B_{66}([R_x^{xy}]^T + [R_y^{xx}])$$

$$[K^{44}] = D_{11}[S^{xx}] + D_{16}([S^{xy}] + [S^{xy}]^T) + D_{66}[S^{yy}] +$$

$$A_{55}[S],$$

$$[K^{45}] = D_{12}[S^{xy}] + D_{16}[S^{xx}] + D_{26}[S^{yy}] + D_{66}[S^{xy}]^T +$$

$$+ A_{45}[S] = [K^{54}]^T,$$

$$[K^{55}] = D_{26}([S^{xy}] + [S^{xy}]^T) + D_{66}[S^{xx}] + D_{22}[S^{yy}] +$$

$$+ A_{44}[S].$$

and

$$S_{ij} = \int_{R^e} \frac{\partial \phi_i}{\partial \xi} \frac{\partial \phi_j}{\partial \eta} \, dxdy \ , \quad \xi,\eta = 0,x,y, \quad S_{ij}^{oo} \equiv S_{ij},$$

$$R_{\zeta}^{\xi\eta} = \int_{R^e} \frac{1}{2} \left(\frac{\partial w}{\partial \zeta}\right) \frac{\partial \phi_i}{\partial \xi} \frac{\partial \phi_j}{\partial \eta} \, dxdy, \quad \zeta,\xi,\eta = 0,x,y,$$

$$\bar{N}_1 = A_{11} \left(\frac{\partial w}{\partial x}\right)^2 + A_{12} \left(\frac{\partial w}{\partial y}\right)^2 + 2A_{16} \frac{\partial w}{\partial x} \frac{\partial w}{\partial y} \ ,$$

$$\bar{N}_2 = A_{12} \left(\frac{\partial w}{\partial x}\right)^2 + A_{22} \left(\frac{\partial w}{\partial y}\right)^2 + 2A_{26} \frac{\partial w}{\partial x} \frac{\partial w}{\partial y} \ ,$$

$$\bar{N}_6 = A_{16} \left(\frac{\partial w}{\partial x}\right)^2 + A_{26} \left(\frac{\partial w}{\partial y}\right)^2 + 2A_{66} \frac{\partial w}{\partial x} \frac{\partial w}{\partial y} \ .$$

SECURITY CLASSIFICATION OF THIS PAGE (When Data Entered)

REPORT DOCUMENTATION PAGE

READ INSTRUCTIONS BEFORE COMPLETING FORM

1. REPORT NUMBER: VPI-E-81-12
2. GOVT ACCESSION NO.: AD-A098913
3. RECIPIENT'S CATALOG NUMBER: (9)

4. TITLE (and Subtitle): (6) ANALYSIS OF LAYERED COMPOSITE PLATES ACCOUNTING FOR LARGE DEFLECTIONS AND TRANSVERSE SHEAR STRAINS.

5. TYPE OF REPORT & PERIOD COVERED: Interim rept.

6. PERFORMING ORG. REPORT NUMBER: Tech. Report No. 21

7. AUTHOR(s): (10) J. N. Reddy

8. CONTRACT OR GRANT NUMBER(s): (15) N00014-78-C-0648 AFOSR-81-0142

9. PERFORMING ORGANIZATION NAME AND ADDRESS: Virginia Polytechnic Institute and State University, Blacksburg, VA 24061

10. PROGRAM ELEMENT, PROJECT, TASK AREA & WORK UNIT NUMBERS: NR064-609

11. CONTROLLING OFFICE NAME AND ADDRESS: Department of the Navy, Office of Naval Research, Structural Mechanics Program (Code 474), Arlington, VA 22217

12. REPORT DATE: May 1981

13. NUMBER OF PAGES: (12) 52

14. MONITORING AGENCY NAME & ADDRESS (if different from Controlling Office)

15. SECURITY CLASS. (of this report): Unclassified

15a. DECLASSIFICATION/DOWNGRADING SCHEDULE

16. DISTRIBUTION STATEMENT (of this Report)

This document has been approved for public release and sale; distribution unlimited

17. DISTRIBUTION STATEMENT (of the abstract entered in Block 20, if different from Report)

18. SUPPLEMENTARY NOTES

A portion of this report will appear as an ASME paper to be presented at the 1981 ASME Vibration Conference, in Hartford, Connecticut during September 15-20, 1981. The paper will appear in its entirity in "Recent Advances in Nonlinear Computational Mechanics," Hinton et al. (eds.), Pine Ridge Press, Swansea, United Kingdom.

19. KEY WORDS (Continue on reverse side if necessary and identify by block number)

angle-ply, composite materials, cross-ply, fiber-reinforced materials, finite element method, free vibration, laminates, large deflections, natural frequencies, nonlinear frequencies, plate bending, rectangular plates, rotatory inertia, transverse shear deformation.

20. ABSTRACT (Continue on reverse side if necessary and identify by block number)

A finite-element analysis is presented for large-deflection bending and large-amplitude free vibration of rectangular plates of cross-ply and angle-ply construction under various edge conditions and loadings. The finite element employed in the present study accounts for transverse shear and rotatory inertia (in the Reissner-Mindlin sense), and large rotations (in the von Karman sense). The finite element solutions are found to agree very closely with results available in the literature.

DD FORM 1 JAN 73 1473 EDITION OF 1 NOV 68 IS OBSOLETE S/N 0102-014-6601

UNCLASSIFIED 268050

SECURITY CLASSIFICATION OF THIS PAGE (When Data Entered)


DA
FILM
6-